Geomechanics and Engineering, *Vol. 39, No. 5 (2024) 483-501*
https://doi.org/10.12989/gae.2024.39.5.483

Wave propagation analysis of composite beams reinforced with nonlinear FG-CNT distributions supported on Kerr elastic foundation utilizing an improved integral first-order shear deformation theory

Saeed Al-Houri[1], Mohammed A. Al-Osta[1,2], Qais Gawah[1], Fouad Bourada[3], Abdelouahed Tounsi*[1,2,3], Salah U. Al-Dulaijan[1] and Abdeldjebbar Tounsi[4]

[1]*Department of Civil and Environmental Engineering, King Fahd University of Petroleum & Minerals, 31261 Dhahran, Eastern Province, Saudi Arabia*
[2]*Interdisciplinary Research Center for Construction and Building Materials, KFUPM, 31261 Dhahran, Saudi Arabia*
[3]*Material and Hydrology Laboratory, University of Sidi Bel Abbes, Faculty of Technology, Department of Civil Engineering, Algeria*
[4]*Department of Mechanical Engineering, Faculty of Science and Technology, University of Rélizane, Algeria*

(*Received June 4, 2024, Revised November 19, 2024, Accepted November 28, 2024*)

Abstract. Functionally graded carbon nanotubes-reinforced composite (FG-CNTRC) has demonstrated a substantial promise for developing advanced lightweight structures and multifunctional composites, a crucial part of modern life, such as in the automotive, aerospace, marine, and medical industries. This work investigates the wave propagation behavior of FG-CNTRC beams resting on an elastic foundation with four configuration patterns of single-walled carbon nanotubes (SWCNTs). The key innovations in this study include nonlinear distributions of FG-CNTs based on exponential power-law models to achieve an optimal distribution of CNTs within the matrix, a Kerr substrate to illustrate the impact of the surroundings, and an improved integral first-order shear deformation theory (FSDT) to analytically formulate the dispersion of the waves with a novel correction function describing the distribution of shear stresses and strains. The rule of mixture is employed in estimating the elastic material's properties, and the governing equations of motion are derived using Hamilton's principle. The results are compared to those found in the literature for validation of the models. The parametric investigation includes the influence of the CNT's dispersion patterns and volume fraction on wave propagation responses. In addition, the study examines the effects of the Kerr foundation and the nonlinear models on wave dispersion behavior. Analytical findings suggest that the arrangements of CNTs manipulate the rigidities of the beams, affecting the dispersion relations. Also, increasing the volume fractions of CNTs improves the stiffness of the beams, corresponding to faster wave velocities. Further, the nonlinear distributions of FG-CNTs greatly influence the wave propagation, depending on the wave type and the patterns of CNTs. Moreover, the foundation presence boosts wave velocities and influences only the bending waves.

Keywords: carbon-nanotube; functionally graded beams; integral first order; Kerr foundation; nonlinear distribution; shear theory; wave propagation

1. Introduction

Carbon nanotubes (CNTs) represent a groundbreaking development in materials science, distinguished by their exceptional mechanical, electrical, and thermal characteristics (Iijima 1991, Saito *et al.* 1998, Dresselhaus *et al.* 2001). First discovered by Iijima in 1991, CNTs consist of graphene sheets rolled into cylindrical or tube-like shapes, yielding a structure with impressive strength, rigidity, and conductivity. The outstanding mechanical characteristics of CNTs include Young's modulus exceeding 1 TPa and tensile strength reaching up to 200 GPa, making them significantly stronger than traditional materials like steel while remaining incredibly lightweight (Ruoff and Lorents 1995, Wong *et al.* 1997). Owing to these properties, CNTs are widely applied in nanoelectronics, aerospace, and biomedical fields (Ajayan and Tour 2007, Bosi *et al.* 2012).

They are especially valuable for reinforcing composites by improving mechanical and thermal performance without adding weight (Thostenson *et al.* 2001, Moniruzzaman and Winey 2006, Alibeigloo 2013). The high electrical conductivity of CNTs makes them suitable for nano-electromechanical systems (NEMS) and advanced sensor applications (Tans *et al.* 1997, Kong *et al.* 2000, Kim and Kuljanishvili 2023). Drawing inspiration from the idea of functionally graded materials (FGMs), Shen first suggested functionally varying the distributions of CNTs within the polymer to enhance the interfacial bonding strength, leading to the creation of a functionally graded carbon nanotube-reinforced composite (FG-CNTRC) (Niino and Maeda 1990, Shen 2009). Notably, FG-CNTRC has attracted interest in achieving customizable properties, enhancing stress distribution, and expanding multifunctionality, which is beneficial in diverse engineering industries (Soni *et al.* 2022). FG-CNTRC enables fine-tuning of thermal and mechanical properties, which pave the way for developing advanced materials with applications in aerospace structural

*Corresponding author, Professor
E-mail: tou_abdel@yahoo.com

ISSN: 2005-307X (Print), 2092-6219 (Online)

parts, pressure vessel valves, acoustics, submarines, rockets, robotics, structural health monitoring, energy harvesting, and biomedical devices where gradients of CNTs can enhance performance (Bharti and Gupta 2013, Dai *et al.* 2019, Ebrahimi *et al.* 2021). Therefore, several researchers investigated the static and dynamic responses of the FG-CNTRC structures.

In recent years, the bending behaviors of the FG-CNTRC beams, plates, arches, and shells have been extensively researched and investigated. Regarding nonlinear bending responses, Zhang *et al*. (2020) analyzed FG-CNTRC shallow arches resting on elastic substrates under uniform radial pressure. The arches had either pinned or clamped ends. The Reddy shear deformation theory (RSDT) and von Karman formulation formed the basis of the analysis. Another study (Shen *et al.* 2020) investigated the nonlinear bending response of the FG-CNTRC plate resting on elastic foundations in a thermal environment by considering a negative Poisson ratio. The temperature-dependent properties of the material were estimated by employing Voigt models. The negative Poisson ratio considerably influenced the bending behavior of the FG-CNTRC plates. By applying a numerical technique, the large deflection solution, as well as the dimensionless load-deflection behaviors of the FG-CNTRC plate, were introduced by Cho (2022). The problem formulation was based on the nonlinear theory of von Karman and a hierarchical model. The introduction of CNTs led to a considerable reduction in central deflection, which became more pronounced with higher volume fractions of CNTs. In another research, Kumar and Sarangi (2022) analyzed bending in the smart FG-CNTRC beam coupled with piezoelectric materials. Throughout the thickness of the beam, there was a variation in the material characteristics, which were determined using the mixture rule. The smart FG-CNTRC beam was analyzed by developing a finite element model. The results revealed that combined piezoelectric materials had a direct impact on the bending responses.

Recently, a considerable focus has been on the dynamic and static behaviors of FG-CNTRC structures. For example, Singh and Sahoo (2021) collaborated to investigate the static and free vibration responses of the FG-CNTRC sandwich plate using the trigonometric shear deformation theory (TSDT) and Navier method. The parametric study detailed the deflection, stress, frequency, volume fraction, and dispersion of CNTs in the FG-CNTRC sandwich plate. Utilizing the first-order discrete layer formulation and the Navier approach, the dynamic properties of the FG-CNTRC sandwich plate containing a viscoelastic core were analyzed by Zhai *et al*. (2021) considering a total of five different stacking sequences. The kinematic relations were derived using the first-order shear deformation theory (FSDT), and then the governing equations were obtained using the Hamilton principle. Furthermore, the vibration frequencies resulting from various stacking sequences were investigated to obtain the best dynamic properties. Arani *et al.* (2014) studied the vibration and instability of CNTRC microtubes visco-elastically coupled and convey fluid. Single-walled carbon nanotubes (SWCNTs) were arranged longitudinally within a poly methyl methacrylate matrix, with the coupled system subjected to a longitudinal magnetic field. The visco-Pasternak foundation was used to capture significant effects of damping and shear, while microtube properties were derived from Mori–Tanaka theory. The model was refined with strain gradient theory incorporated in a Timoshenko beam model. The motion equations, derived via Hamilton's principle and solved with the differential quadrature method, analyzed the impacts of factors like volume fractions of CNTs, magnetic intensity, Knudsen number, and elastic medium on vibration characteristics. In another article by Chen *et al.* (2022), the dynamic instability analysis of the FG-CNTRC hybrid plate under periodic loads was presented in detail. The Galerkin approach with a reduced eigenfunction transform derived the governing equations (Mathieu-form). The outcomes revealed the significant impact of the CNT's volume fraction, dynamic loading, and bending stresses on the dynamic instability. By employing the TSDT, research was carried out by Chaikittiratana and Wattanasakulpong (2022) to analyze the dynamic behaviors of the FG-CNTRC beam subjected to different dynamic loadings. The obtained governing equations were solved using the Gram-Schmidt-Ritz technique. Moreover, the Newmark integration was utilized to investigate the beam's dynamic responses when subjected to dynamic loadings. In another study, Houalef *et al.* (2023) examined the free vibration behavior of the FG-CNTRC beam according to a refined third-order shear deformation finite element (FE) beam theory. Lagrange's approach obtained the governing differential equations and then solved them numerically using the differential quadrature finite element method (QFEM). A recent article by Chalak *et al.* (2023) conducted a study on the free vibration behaviors of the FG-CNTRC beam exposed to a hygro-thermal environment. The analysis followed the FE high-order zigzag theory and employed temperature-dependent material properties. A total of five distribution patterns of CNTs were considered. The CNT's gradation rule significantly affected the stress dispersion throughout the beam's thickness. In recent research, Ong *et al.* (2023) analyzed the vibration responses of the porous viscoelastic FG-CNTRC beam. Furthermore, simply supported beams with four distribution patterns of CNTs and three porosity models were considered in the study. The derivation of the governing equations was done through an energy method that considered the viscoelastic beams and layers. Then, those equations were solved using a proposed series expansion approach. Zhang *et al.* (2023a) investigated analytically the elastic stability of the imperfect FG plates embedded between CNTRC piezoelectric patches exposed to hygrothermal environment via a novel quasi 3D-HSDT. Liu *et al.* (2023) analyzed the nonlinear dynamic response of curved pipes with temperature-dependent properties via higher order shear deformation theory. Based on HSDT theory and Navier's method, Ozbey *et al*. (2024) investigates the vibrational behaviour of FG-CNT-viscoelastic reinforced composite plate under dynamic loading. Haghparast (2020) proposed a theoretical vibration analysis of fluid-floating axially moving sandwich plates consisting of a balsa wood core and two nanocomposite

face sheets. The study examined the effects of fluid-structure interaction (FSI) on the stability of the plates in both ideal and viscous fluids. The Halpin–Tsai model was applied to estimate the material properties of randomly oriented and uniformly distributed CNTs within a matrix. The governing equations were formulated using sinusoidal shear deformation plate theory (SSDT), which does not require a corrective shear factor. The motion equations were derived using Hamilton's principle and solved via a semi-analytical approach. Results revealed that the dimensionless frequencies decline significantly as water levels rise and become almost constant for fluid levels above 50% of the plate length.

Recently, some researchers have focused on wave propagation analysis of various structures as it has a lot of practical applications. For instance, wave dispersion is crucial in predicting the responses of systems to distinct loading scenarios (Gopalakrishnan and Narendar 2013). Moreover, the aerospace and military commonly apply the wave propagation principle when analyzing the long-term damage to CNT composites resulting from extreme loadings. Additionally, it is considered among the most effective techniques for examining the fracture's dispersion. Furthermore, the vibration responses result basically from wave propagation, which is highly significant for the mechanical behavior analysis of the structure. Seyfi *et al.* (2022) introduced a study examining the wave propagation behavior in an FG-CNTRC beam placed on a Winkler-Pasternak elastic substrate. The gradation of CNTs was applied throughout the thickness of the beam following a power-law formulation. Modeling the FG-CNTRC beams resting on elastic foundations was based on the Euler-Bernoulli beam theory, while the governing equations were derived using the Hamilton principle. Using the second-order shear deformation theory (SSDT), Janghorban and Nami (2017) analyzed wave propagation in FG-CNTRC plates. A total of four distribution patterns were accounted for in the study. An analytical approach was used to obtain the frequency and phase velocity. A recent article by Hao and Li (2023) presented the wave dispersion analysis of infinite piezoelectric FG-CNTRC sandwich plates. The kinematic governing equations were derived by applying the TSDT and Hamilton principles. In (Ebrahimi and Rostami 2018a), the wave propagation behaviors of FG-CNTRC beams were investigated, resting on a Winkler elastic foundation in thermal environments by applying various shear deformation theories. The wave dispersion analysis of the FG-CNTRC beams supported by a Winkler elastic substrate was conducted in (Ebrahimi and Rostami 2018b), considering four different reinforcement patterns. The governing equations were derived from the Hamilton principle and then solved analytically. Hosseini *et al*. (2023) investigated the small-scale effect on the wave propagation characteristics of FG carbon nanotube-reinforced composite nanoplates using first-order shear deformation theory (FSDT) and nonlocal strain gradient theory. Based on the higher order shear deformation theory, Ding *et al.* (2023) investigated the thermal environment effect on the wave propagation of the FG-CNTRC with including the material properties size dependent effect. In recent research (Zhang *et al.* 2023b), by applying HSDT, the wave propagation behaviors of the FG-CNTRC beam supported by Winkler and Winkler-Pasternak elastic foundations were investigated. The Euler-Lagrange approach was employed to obtain the governing equations, which were then solved using the eigenvalue technique.

Based on the literature review, there are some notable gaps in the wave propagation analysis of FG-CNTRC beams, including limited research compared to buckling, vibration, and bending studies, an absence of different foundation models besides Winkler and Winkler-Pasternak foundations, reliance on linear distribution models of CNTs, and an emphasis on bending waves while overlooking longitudinal and shear waves, with no prior use of an FSDT with integral form. Therefore, for the first time, this paper analyzes the wave propagation behavior of the FG-CNTRC beams supported on the Kerr substrate based on a nonlinear distribution of CNTs and an integral FSDT. A novel correction function was proposed for the shear strain to enhance the accuracy of the results. The proposed model is validated by comparing its outcomes with the results found in the literature. The elastic constituent's properties were determined using the mixture rule, while the Hamilton principle derived the governing equations of motion. The study examines how the models of CNTs and Kerr foundation coefficients influence the wave dispersion responses.

2. Mathematical model of an FG-CNTRC beam

2.1 Configuration and properties of the beam

Fig. 1 illustrates a beam with a uniform (UD) distribution of CNTs, supported by a Kerr foundation, with a thickness (h) and a length (L). The foundation parameters are k_U, k_s and k_L, which represent the upper, shear, and lower layer coefficients, respectively.

The FG-CNTRC beams are created using a mixture of SWCNTs and polymer matrix. This study assumes different nonlinear forms of CNTs' distribution across the beams' cross-sections: FG-O, FG-X, and FG-V, as demonstrated in Table 1.

For the case of (n = 0), the distribution of CNTs becomes uniform in the polymer matrix, resulting in the UD Beam, as shown in Fig. 1. The mathematical functions that describe the patterns of CNTs are defined in terms of exponential power-law volume fractions of CNTs, as illustrated in Table 2 (Zerrouki *et al.* 2021).

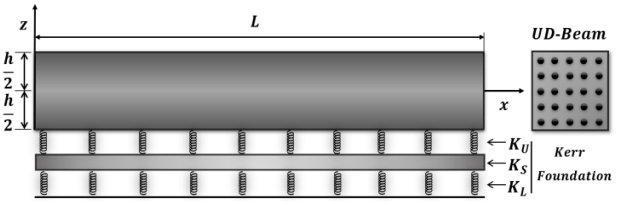

Fig. 1 Geometry of a UD beam in Kerr foundation

Table 1 Cross-sections of nonlinear types of CNTs

Distribution of CNTs	$0 < n < 1$	$n = 1$	$1 < n$
FG-O	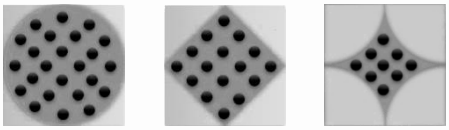		
FG-X	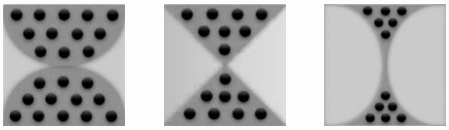		
FG-V	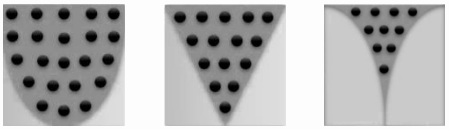		

Table 2 Expressions of CNTs' patterns distributed along the beam thickness

CNT's Patterns	V_{cnt}	
UD	$V_{cnt} = V_{cnt}^{*}$	(1a)
FGO	$V_{cnt} = (n+1)\left(1 - 2\frac{\lvert z\rvert}{h}\right)^{n} V_{cnt}^{*}$	(1b)
FGX	$V_{cnt} = (n+1)\left(2\frac{\lvert z\rvert}{h}\right)^{n} V_{cnt}^{*}$	(1c)
FGV	$V_{cnt} = (n+1)\left(\frac{1}{2} + \frac{z}{h}\right)^{n} V_{cnt}^{*}$	(1d)

where:

n: The exponent degree of the power-law distributions of CNTs.

V_{cnt}^{*}: The given volume fraction of CNTs, which is computed as:

$$V_{cnt}^{*} = \frac{W_{cnt}}{W_{cnt} + \left(\frac{\rho^{cnt}}{\rho^{p}}\right)(1 - W_{cnt})} \tag{2}$$

where:

W_{cnt}: The mass fraction of CNTs.

ρ^{cnt}, ρ^{p}: The density of CNTs and the polymer matrix, respectively.

The relationship between the volume fractions of the CNTs and matrix polymer in Eq. (3) holds for each position of the beam

$$V_{cnt} + V_p = 1 \tag{3}$$

where:

V_p: The volume fraction of the polymer matrix.

The micromechanical model known as the law of mixture is employed to assess the effective material properties of FG-CNTRC beams. The following is an expression for the material properties (Jenabi *et al.* 2024)

$$E_{11} = \eta_1 V_{cnt}\, E_{11}^{cnt} + V_p\, E^{p} \tag{4}$$

$$\frac{\eta_2}{E_{22}} = \frac{V_{cnt}}{E_{22}^{cnt}} + \frac{V_p}{E^{p}} \tag{5}$$

$$\frac{\eta_3}{G_{12}} = \frac{V_{cnt}}{G_{12}^{cnt}} + \frac{V_p}{G^{p}} \tag{6}$$

where:

E_{11}^{cnt}, E_{22}^{cnt}, and E^{p}: The Young's modulus of CNTs and the polymer, respectively.

G_{12}^{cnt} and G^{p}: The shear modulus of CNTs and polymer, respectively.

η_1, η_2, and η_3 : The efficiency coefficients of CNTs considering the size-dependent characteristics of SWCNTs.

By utilizing the same rule, the Poisson's ratio and the density of the FG-CNTRC beams are expressed as

$$v = V_{cnt} v^{cnt} + V_p v^{p} \tag{7}$$

$$\rho = V_{cnt} \rho^{cnt} + V_p \rho^{p} \tag{8}$$

where:

v^{cnt} and v^{p} : The Poisson's ratios of CNTs and the polymer, respectively.

2.2 The Kerr foundation

The surrounding medium of a structure affects its behavior based on the contact mechanics of the underlying materials with the structural components (Yaylaci *et al.* 2022a, b, Adiyaman *et al.* 2023).

This study aims to analyze the response of the FG-CNTRC beam placed on a Kerr foundation that implements three different actions: the upper and lower spring layers actions and the shear interaction, as shown in Fig. 1. Thus, the foundation effect can be implemented based on the transverse middle displacement w_0 as (Kerr 1965, Birgani *et al.* 2024)

$$R_f = \left(\frac{k_L\, k_U}{k_L + k_U} w_0(x,t) - \frac{k_s\, k_U}{k_L + k_U} \nabla^2 w_0(x,t)\right) \tag{9}$$

where:

R_f: The reaction force of the foundation.

∇^2: The Laplace operator.

k_L, k_U, and k_s: The parameters of the lower spring, upper spring, and shear layer, respectively.

$f_{\underbrace{i}_{\overbrace{xxx}}\ \underbrace{j}_{\overbrace{yyy}}}$: It indicates a derivate of function f with respect to some variable $\left(\frac{\partial^{(i+j)} f}{\partial x^{(i)} \partial y^{(j)}}\right)$. The repeated symbols represent higher-order derivatives for each variable.

The Winkler-Pasternak foundation emerges when the upper layer becomes infinitely stiff, which is equivalent to its removal. Thus, the reaction force becomes as follows

$$R_f = \left(k_L\, w_0(x,t) - k_s\, w_{0,xx}(x,t)\right) \tag{10}$$

To facilitate the discussion and comparisons, the foundation parameters are defined as the following

$$k_U = \beta_U \left(\frac{A_{110}}{L^2}\right), \qquad k_L = \beta_L \left(\frac{A_{110}}{L^2}\right) \tag{11}$$

$$k_s = \beta_s\, A_{110} \tag{12}$$

Where:

β_L, β_U, and β_s: The constant factors of the lower spring, upper spring, and shear layer, respectively.

3. Theoretical formulations

3.1 Kinematics

Based on Timoshenko's theory, an improved integral FSDT is used to describe the beam behavior. The simple FSDT with integral form offers significant benefits by incorporating a single undetermined integral term in the displacement field, which reduces complexity and effectively enables more precise shear rotations. The displacement field involves u_0, w_0, and θ as the unknowns, expressed as follows

$$u = u_0(x,t) - z\,k_1 \int \theta(x,t)dx \qquad w = w_0(x,t) \tag{13}$$

where:

$u_0(x,t), w_0(x,t)$: The middle-plane displacements ($z = 0$) in the x and z directions, respectively.

$\theta(x,t)$: The beam rotation.

3.2 Strain-displacement relations

The linear strain-displacement relationships are used to derive the components of the strains in terms of displacement unknowns. The indicial notation in Eq. (14) expresses the 3D infinitesimal strain for small deformation as follows

$$\varepsilon_{ij} = \frac{1}{2}\left(u_{i,x_j} + u_{j,x_i}\right), \qquad i,j = 1,2,3. \qquad \{u_1,u_2,u_3\} = \{u,v,w\}, \qquad \{x_1,x_2,x_3\} = \{x,y,z\} \tag{14}$$

The components of strains contain only ε_x and γ_{xz} based on the assumptions of the displacement fields, derived as follows

$$\varepsilon_x = u_{,x} = u_{0,x} - z\,k_1\,\theta \tag{15}$$

$$\gamma_{xz} = C_f\left(u_{,z} + w_{0,x}\right) = C_f\left(w_{0,x} - k_1 \int \theta dx\right) \tag{16}$$

where:

C_f : The shear correction function. In the present investigation, a novel corrective function is taken in a trigonometric form, expressed in Eq. (17)

$$C_f = \frac{\pi}{r}\cos\left(\frac{\pi\,z}{h}\right) \qquad r = 2.425 \tag{17}$$

Applying the analytical solution of wave propagation simplifies the undetermined integrals to the relation illustrated in Eq. (18)

$$\int \theta(x,t)dx = A'\frac{\partial\theta(x,t)}{\partial x} \tag{18}$$

where A' and k_1 are related as functions of the wavenumber λ as follows

$$A' = -\frac{1}{\lambda^2}, \qquad k_1 = \lambda^2 \tag{19}$$

The characteristics of the exponential functions employed in the general wave propagation solution led to this simplification.

3.3 Stress-strain relations

The constitutive relations are used to determine the stresses, expressed in Eq. (20) as a matrix form

$$\{\sigma\} = [Q]\{\varepsilon\} \tag{20}$$

where:

[Q]: The stiffness matrix.

{σ} and {ε}: The stress and strain vectors, respectively.

Based on the assumptions, the only relevant stresses for this study are σ_x and τ_{xz}, which correspond to non-zero components of the strains, defined as the following

$$\sigma_x = Q_{11}(z)\,\varepsilon_x, \qquad \tau_{xz} = Q_{55}(z)\,\gamma_{xz} \tag{21}$$

$$Q_{11}(z) = \frac{E_{11}(z)}{1-\nu(z)^2}, \qquad Q_{55}(z) = G_{12}(z) \tag{22}$$

3.4 Governing equations

The motion equations are derived based on the Hamilton's principle, stated as (Avcar 2019, Akbas 2015, Al-Basyouni *et al.* 2020, Selmi 2020, Arani *et al*. 2020, Zhu 2023, Xiao 2023, Long *et al*. 2023, Gan *et al*. 2023, Sahoo *et al.* 2023):

$$\int_{t_1}^{t_2} (\delta U + \delta V - \delta K)dt = 0 \tag{23}$$

where:

δ: The first variation operator.

$U, V, and\ K$: The strain energy, work of the external forces, and the kinetic energy, respectively.

The three unknown middle-plane displacements are used to express the energy variations.

The strain energy variation is found as follows

$$\delta U = \int_0^L \int_{-h/2}^{h/2} (\sigma_x \delta\varepsilon_x + \tau_{xz}\delta\gamma_{xz})\,dz\,dx = \int_0^L \left(N\,\delta u_{0,x} - k_1\,M_b\,\delta\theta + Q\left(\delta w_{0,x} - A'\,k_1\,\delta\theta_{,x}\right)\right)dx \tag{24}$$

where:

N, M_b, and Q: The stress resultants, expressed as

$$\begin{Bmatrix} N \\ M_b \end{Bmatrix} = \int_{-h/2}^{h/2} \sigma_x \begin{Bmatrix} 1 \\ z \end{Bmatrix} dz\,, \qquad Q = \int_{-h/2}^{h/2} \tau_{xz}\,dz \tag{25}$$

The virtual external work done by the Kerr foundation can be written as

$$\delta V = \int_0^L \left(\frac{k_L\,k_U}{k_L + k_U} w_0 - \frac{k_s\,k_U}{k_L + k_U} w_{0,xx}\right)\delta w_0\,dx \tag{26}$$

The variation of kinetic energy takes the following form

$$\begin{aligned}\delta K = \int_0^{\mathrm{L}} \int_{-h/2}^{h/2} \rho(z)\,(\dot{u}\,\delta\dot{u} + \dot{w}_0\,\delta\dot{w}_0)\,dz\,dx \\ = -\int_0^{\mathrm{L}} \int_{-h/2}^{h/2} \rho(z)\,(\ddot{u}\,\delta u \\ + \ddot{w}_0\,\delta w_0)\,dz\,dx\end{aligned} \tag{27}$$

By expanding and simplifying, it could be written as represented in Eq. (28)

$$\begin{aligned}\delta K = -\int_0^{\mathrm{L}} \big(I_0(\ddot{u}_0\,\delta u_0 + \ddot{w}_0\,\delta w_0) \\ - I_1\big(A'\,k_1\,\ddot{w}_0\,\delta\theta_{,x} + A'\,k_1\,\delta\ddot{\theta}_{,x}\,\delta u_0\big) \\ + I_2\,(A'\,k_1)^2\,\delta\ddot{\theta}_{,x}\,\delta\theta_{,x}\big)\,dx\end{aligned} \tag{28}$$

where:

$\overset{i}{\dddot{f}}$: It indicates a derivate of function f with respect to the time $\left(\frac{\partial^{(i)} f}{\partial t^{(i)}}\right)$. The repeated dots indicate higher-order derivatives.

$I_i\ (i = 0, 1, 2)$: The mass inertia terms, expressed as

$$\begin{Bmatrix} I_0 \\ I_1 \\ I_2 \end{Bmatrix} = \int_{-h/2}^{h/2} \rho(z) \begin{Bmatrix} 1 \\ z \\ z^2 \end{Bmatrix} dz \tag{29}$$

The motion equations are then determined with the use of the calculus of variations when the energy virtual variations (δU, δV, and δK) in Eqs. (24), (26), and (28) are substituted into Hamilton's principle as functions of the three middle displacements. After integrating by parts and setting the coefficients of δu_0, δw_0, and δθ to zero, the following three equations are finally obtained

$$\begin{aligned}&\delta u_0\colon\ N_{,x} = I_0\,\ddot{u}_0 - I_1\,A'\,k_1\,\ddot{\theta}_{,x} \\ &\delta w_0\colon\ Q_{,x} - \frac{k_L\,k_U}{k_L + k_U} w_0 + \frac{k_s\,k_U}{k_L + k_U} w_{0,xx} = I_0\,\ddot{w}_0 \\ &\delta\theta\colon\ M_b\,k_1 - Q_{,x}\,A'\,k_1 \\ &\qquad = I_1\,A'\,k_1\,\ddot{u}_{0,x} - I_2\,(A'\,k_1)^2\,\ddot{\theta}_{,xx}\end{aligned} \tag{30}$$

The expression of the stress resultants in the motion equations as a combination of displacements and material stiffness components is shown in Eq. (31)

$$\begin{aligned}\begin{Bmatrix} N \\ M_b \end{Bmatrix} = \begin{bmatrix} A_{11} & B_{11} \\ B_{11} & D_{11} \end{bmatrix} \begin{Bmatrix} u_{0,x} \\ -k_1\theta \end{Bmatrix} \\ Q = A_{55}\left(w_{0,x} - A'\,k_1\,\theta_{,x}\right)\end{aligned} \tag{31}$$

where:

A_{11}, B_{11}, D_{11}, and A_{55}: The stiffnesses of the beam, defined as

$$\begin{aligned}\begin{Bmatrix} A_{11} \\ B_{11} \\ D_{11} \end{Bmatrix} = \int_{-h/2}^{h/2} Q_{11} \begin{Bmatrix} 1 \\ z \\ z^2 \end{Bmatrix} dz\,, \\ A_{55} = \int_{-h/2}^{h/2} {C_f}^2\,Q_{55}\,dz\end{aligned} \tag{32}$$

After substituting the resultants-displacements relations, the governing equations are obtained in Eq. (33) as functions of the middle displacements only

$$\begin{aligned}\mathrm{A}_{11}\,u_{0,xx} - B_{11}k_1\,\theta_{,x} = I_0\,\ddot{u}_0 + I_1\ddot{\theta}_{,x} \\ A_{55}\left(w_{0,xx} + \theta_{,xx}\right) - \frac{k_L\,k_U}{k_L + k_U} w_0 + \frac{k_s\,k_U}{k_L + k_U} w_{0,xx} \\ = I_0\,\ddot{w}_0 \\ B_{11}\,k_1\,u_{0,x} - D_{11}\,{k_1}^2\,\theta + A_{55}\left(w_{0,xx} + \theta_{,xx}\right) \\ = -I_1\,\ddot{u}_{0,x} + I_2\,\ddot{\theta}_{,xx}\end{aligned} \tag{33}$$

3.5 Dispersion relations

The analytical solutions of the middle-plane displacements for wave propagation in an infinite beam are as follows (Al-Osta 2022, Wu and She 2023)

$$\begin{Bmatrix} u_0(x,t) \\ w_0(x,t) \\ \theta(x,t) \end{Bmatrix} = \begin{Bmatrix} U_m\,e^{i(\lambda\,x - \omega\,t)} \\ W_m\,e^{i(\lambda\,x - \omega\,t)} \\ \theta_m\,e^{i(\lambda\,x - \omega\,t)} \end{Bmatrix} \tag{34}$$

where:

U_m, W_m, and θ_m: The amplitudes of the waves.

i: The imaginary number ($\sqrt{-1}$).

λ: The wavenumber in the x-axis.

ω: The circular frequency.

If the displacement solutions in Eq. (34) are inserted into Eq. (33), an eigenvalue problem is produced, and it can be rewritten as a matrix form like the following

$$([K] - \omega^2[M])\,\{\Lambda\} = 0 \tag{35}$$

where:

$[K]$: The stiffness matrix that contains the work and the strain energy terms.

$[M]$: The mass matrix that contains the kinetic energy terms.

{Λ}: The vector of the waves' amplitudes.

The detailed representations of the matrices' equations in Eq. (35) are expressed as

$$\left(\begin{bmatrix} K_{11} & K_{12} & K_{13} \\ K_{12} & K_{22} & K_{23} \\ K_{13} & K_{23} & K_{33} \end{bmatrix} - \omega^2 \begin{bmatrix} M_{11} & M_{12} & M_{13} \\ M_{12} & M_{22} & M_{23} \\ M_{13} & M_{23} & M_{33} \end{bmatrix}\right) \begin{Bmatrix} U_m \\ W_m \\ \theta_m \end{Bmatrix} = 0 \tag{36}$$

where the following describes the components of the symmetric stiffness matrix

$$\begin{Bmatrix} K_{11} \\ K_{12} \\ K_{13} \\ K_{22} \\ K_{23} \\ K_{33} \end{Bmatrix} = \begin{Bmatrix} A_{11}\lambda^2 \\ 0 \\ i\,B_{11}k_1\lambda \\ -\frac{k_L\,k_U}{k_L + k_U} - \frac{k_s\,k_U}{k_L + k_U}\lambda^2 - A_{55}\,\lambda^2 \\ -A_{55}\,\lambda^2 \\ -D_{11}k_1^2 - A_{55}\,\lambda^2 \end{Bmatrix} \tag{37}$$

and for the elements of the symmetric mass matrix

$$\begin{Bmatrix} M_{11} \\ M_{12} \\ M_{13} \\ M_{22} \\ M_{23} \\ M_{33} \end{Bmatrix} = \begin{Bmatrix} I_0 \\ 0 \\ i\,I_1\,\lambda \\ -I_0 \\ 0 \\ -I_2\,\lambda^2 \end{Bmatrix} \tag{38}$$

This eigenvalue problem has a non-trivial solution only if the determinant of $|[K]-\omega^2[M]|$ is equal to zero. The circular frequencies are numerically solved in terms of wavenumbers by taking the square root of the eigenvalues. There are three circular and wave frequencies, which correlate to the three unknown theory displacements, as indicated below

$$\omega_i = \omega_i(\lambda), \qquad (i = 1, 2, 3) \tag{39}$$

$$f_i(\lambda) = \frac{\omega_i(\lambda)}{2\pi} \tag{40}$$

where ω_1, ω_2, and ω_3 represent the frequencies of bending, longitudinal, and shear wave modes, respectively. The phase velocity C_{pi} and the group velocity C_{gi} are found from the circular frequencies relations

$$C_{pi} = \frac{\omega_i(\lambda)}{\lambda}, \qquad C_{gi} = \frac{d\omega_i(\lambda)}{d\lambda} \tag{41}$$

For validation purposes, the dimensionless circular frequencies are utilized, stated as follows

$$\overline{\omega} = \omega\, L \sqrt{\frac{I_{00}}{A_{110}}} \tag{42}$$

$$I_{00} = \int_{-\frac{h}{2}}^{\frac{h}{2}} \rho^{\rho}\, dz\,, \qquad A_{110} = \int_{-\frac{h}{2}}^{\frac{h}{2}} \frac{E_p}{1-\nu_p^2}\, dz \tag{43}$$

where:

I_{00} and A_{110}: The inertia and stiffness of a beam made completely of a pure polymer matrix, respectively.

4. Numerical results and discussion

This section includes results validation to verify the model's accuracy and parametric studies to investigate the effects of various parameters. The results of the FG-CNTRC beams are based on armchair (10, 10) SWCNTs and polymethyl methacrylate (PMMA), serving as the reinforcement and polymer matrix, respectively. The mechanical properties of the CNTs and matrix are stated in Table 3 (Wattanasakulpong and Ungbhakorn 2013). The CNTs-given volume fractions (V_{cnt}^*) and their associated parameters of efficiency (η_i) are shown in Table 4 (Wattanasakulpong and Ungbhakorn 2013).

4.1 Results validation

The mathematical models have been validated numerically by comparing their outcomes with the free vibration results in previous publications. Table 5 compares the dimensionless fundamental frequency of the present work with that of previous studies conducted by Wattanasakulpong and Ungbhakorn (2013), Tagrara *et al*. (2015), Alsubaie *et al*. (2023), and Gawah *et al*. (2024). The comparisons in Table 5 disregard the nonlinearity of CNTs volume fraction in the current work because the references only consider the linear case with n = 1. The left part in Table 5 presents the fundamental frequency results for beams without foundation, while the right part displays the results for beams supported by the Winkler-Pasternak foundation.

Table 3 Mechanical properties of CNTs and polymer

CNTs	E_{11}^{cnt}	E_{22}^{cnt}	G_{12}^{cnt}	ρ^{cnt}	ν^{cnt}
	600 GPa	10 GPa	17.2 GPa	1400 kg/m^3	0.19
Polymer (PMMA)	E^p	G^p	ρ^p	ν^p	
	2.5 GPa	$\frac{E_p\ GPa}{2(1+\nu_p)}$	1190 kg/m^3	0.3	

Table 4 Volume fractions of CNTs and their respective efficiency parameters

Case	η_1	η_2	η_3
V_{cnt}^* **= 0.12**	1.2833	1.0566	1.0566
V_{cnt}^* **= 0.17**	1.3414	1.7101	1.7101
V_{cnt}^* **= 0.28**	1.3238	1.7380	1.7380

Table 5 indicates that while the present theory comprises an FSDT, it closely matches the more advanced published HSDT theories, showing only minor discrepancies. This accuracy is achieved by incorporating the novel shear correction function, leading to improved results.

Another comparison of the dimensionless fundamental frequency is made with Zerrouki *et al*. (2022), considering the nonlinearity of FG-CNTs, as shown in Table 6, the present study results are relatively similar to those of Zerrouki. Furthermore, as the value of the exponent increases, the fundamental frequency of the X-beam rises while the fundamental frequency of the O-beam and V-beam declines.

4.2 Parametric analysis

This presents a parametric wave propagation analysis of nonlinear FG-CNTs-reinforced composite beam. Several examples are used to study the impacts of CNT's nonlinear arrangement and volume fractions and the Kerr foundation on various dispersion relations.

4.2.1 Effect of CNTs patterns and volume fractions

The wave velocities propagate differently based on the distribution patterns of CNTs. Fig. 2 presents comparison graphs of the nonlinear configurations of CNTs in the FG-CNTRC beams to evaluate the behavior of phase and group velocities.

Fig. 2(a) shows that the phase velocities of the bending waves sharply decrease at first before slightly increasing and stabilizing, while the group velocities increase as the wavenumber grows until reaching peak values and then leveling off. Also, both velocities exhibit a reversal behavior where the beams of higher velocities initially switch to having slightly slower overall velocities. Additionally, at lower wavenumbers, the X-beam has the highest velocities of bending waves, whereas as the wavenumber grows, the O-beam becomes slightly higher.

Table 5 Comparison of the dimension-less fundamental frequencies (L/h = 15, Vcnt = 0.12, $\boldsymbol{\lambda = \frac{\pi}{L}}$)

Theory	$\boldsymbol{\beta_L = \beta_s = 0.0}$				$\boldsymbol{\beta_U = \infty,\ \beta_L = 0.1,\ \beta_s = 0.02}$			
	UD	***O***	***X***	***V***	***UD***	***O***	***X***	***V***
FSDT[(a)]	0.9976	0.7628	1.1485	0.8592	1.1339	0.9339	1.2688	1.0142
TSDT[(a)]	0.9745	0.7453	1.1152	0.8441	1.1137	0.9198	1.2387	1.0014
Ref[(b)]	0.9749	0.7446	1.1163	0.8442	1.1140	0.9192	1.2397	1.0015
Ref[(c)]	0.9750	0.7446	1.1164	0.8444	1.1141	0.9192	1.2399	1.0017
Ref[(d)]	0.9745	0.7554	1.1033	0.8442	1.1137	0.9279	1.2280	1.1015
Present	0.9750	0.7557	1.1035	0.8444	1.1141	0.9282	1.2282	1.0017

FSDT[(a)] and TSDT[(a)] from Wattanasakulpong and Ungbhakorn (2013); Ref[(b)] from Tagrara *et al.* (2015); Ref[(c)] from Alsubaie *et al*. (2023); Ref [(d)] from Gawah *et al.* (2024)

Table 6 Comparison of the dimensionless frequencies with nonlinearity effect (L/h = 15, Vcnt = 0.12, $\boldsymbol{\lambda = \frac{\pi}{L}}$)

	$\boldsymbol{\beta_L = \beta_s = 0.0}$					
	O		***X***		***V***	
	Present	***Ref[(a)]***	***Present***	***Ref[(a)]***	***Present***	***Ref[(a)]***
0.5	0.8529	0.8440	1.0556	1.0609	0.9111	0.9087
1.0	0.7557	0.7453	1.1035	1.1152	0.8444	0.8447
1.5	0.6780	0.6684	1.1352	1.1530	0.7840	0.7875
2.0	0.6153	0.6069	1.1575	1.1812	0.7313	0.7375
2.5	0.5639	0.5569	1.1741	1.2031	0.6861	0.6941

Ref[(a)] from Zerrouki *et al.* (2022)

In longitudinal waves, the phase and group velocity of the V-beam are the only ones that exhibit a declining behavior due to unsymmetric arrangement of CNTs in the matrix, as shown in Fig. 2(b).

In parallel to the behavior of bending waves' velocities, the phase velocities of the shear waves descend sharply as the wavenumber increases before reaching stable values, while the group velocities increase as the wavenumber grows until converging to constant values, as pictured in Fig. 2(c). Besides, the X-beam shows the highest shear wave velocities at lower wavenumbers, but the V-beam rapidly surpasses it at higher wavenumbers.

It can be concluded generally from Fig. 2 that the X-beam exhibits high bending rigidity, whereas the V-beam possesses the highest shear rigidity. Additionally, the symmetric distribution of CNTs does not affect the beam's axial rigidity, while the asymmetric arrangement of the V-beam reduces it.

The volume fractions of CNTs affect the dispersion relations of FG-CNTRC beams. All beams exhibit nearly identical behavior in terms of CNTs volume fractions. Hence, only the X-beam is used to represent the other beams. Fig. 3 illustrates the variation of phase and group velocities with the wavenumber at different volume fractions of CNTs (0.12, 0.17, and 0.28) for the X-beam. Generally, the volume fractions of CNTs do not affect both velocities at low wave numbers, while its impact becomes more pronounced as the wavenumber increases.

As anticipated, it is evident that increasing the volume fractions of CNTs leads to higher wave velocities, thanks to enhanced stiffness and the increase of the material rigidity.

4.2.2 Effect of the nonlinear CNTs distributions

The introduction of the nonlinearity in the arrangements of CNTs affects the wave propagation of beams reinforced with FG-CNT distribution (O-beam, X-beam, V-beam). Only the dispersion relations of V-beam are considered in detail because it is being influenced the most by the exponent degree. Fig. 4 illustrates the dispersion relations of V-beam with different nonlinearity degrees.

Fig. 4(a) shows that the phase and group velocities of the bending waves are affected the most by the exponent degree when the wavenumber is in the range of 0.05 and 1 1/m. Also, as the exponent degree increases, both velocities tend to decline.

The longitudinal waves shown in Fig. 4(b) indicate that the nonlinearity of CNTs has an incredible effect on the wave velocities as the wavenumber increases due to an unsymmetric nature of the V-beam distribution. Furthermore, the phase and group velocities grow and linearize as the values of the exponent degree decrease, approaching the behavior of symmetric beams.

In contrast to bending and longitudinal waves, the phase and group velocities of shear waves rise as the degree of nonlinearity increases. Also, as the wavenumber increases, both velocities increase, as depicted in Fig. 4(c).

The FG-CNTRC beams have different behaviors regarding the effect of the nonlinear distributions of CNTs. In Fig. 5, the relations of the phase and group velocities versus the exponent degree of CNTs are plotted to compare the behavior of each beam type regarding the nonlinearity effect. Also, all curves are based on a wavenumber of 0.3 1/m, with the UD beam being the baseline for comparison of other beams' behaviors.

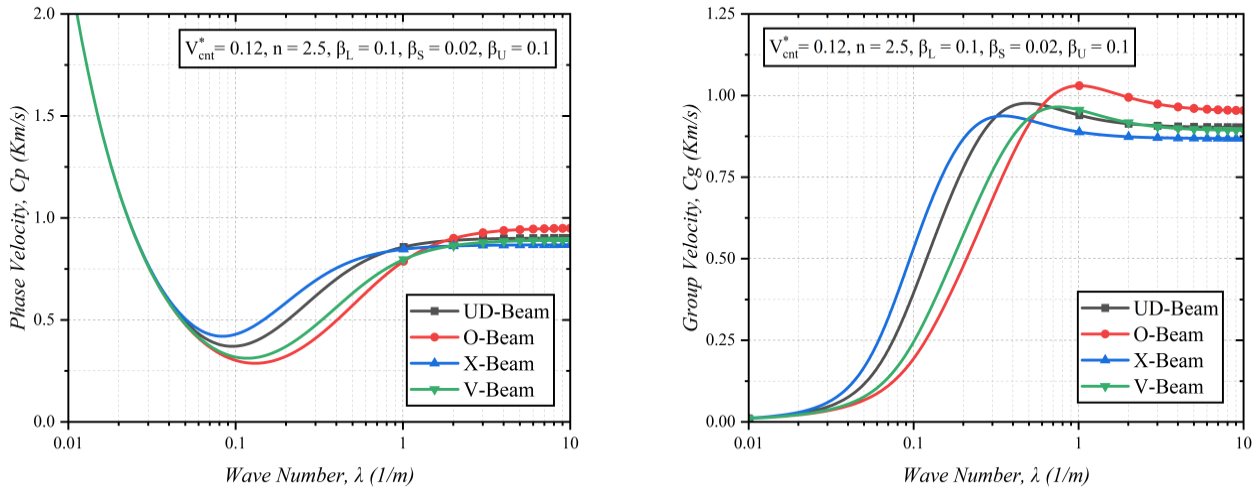

(a) Bending waves

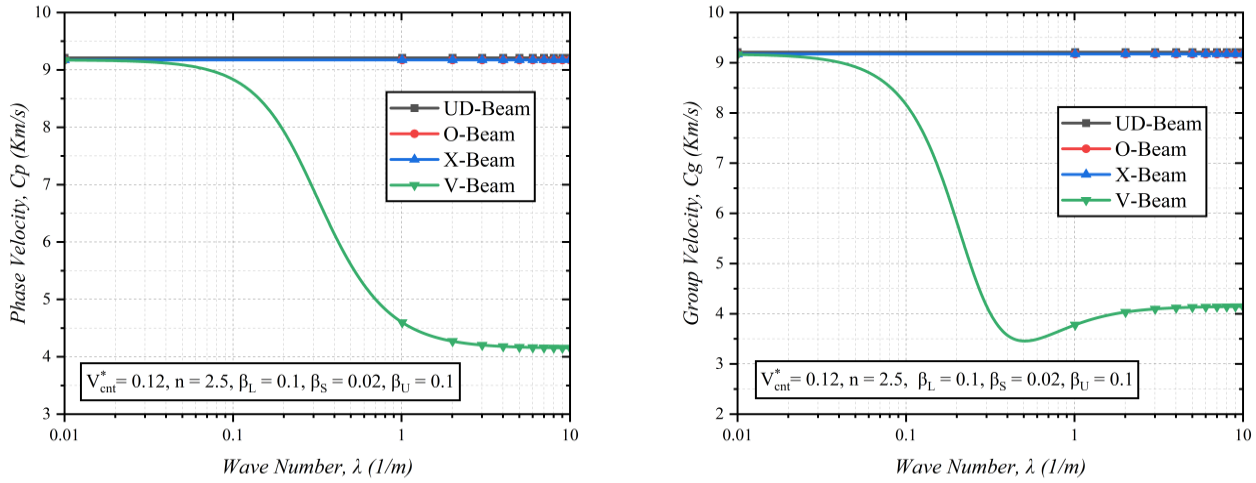

(b) Longitudinal waves

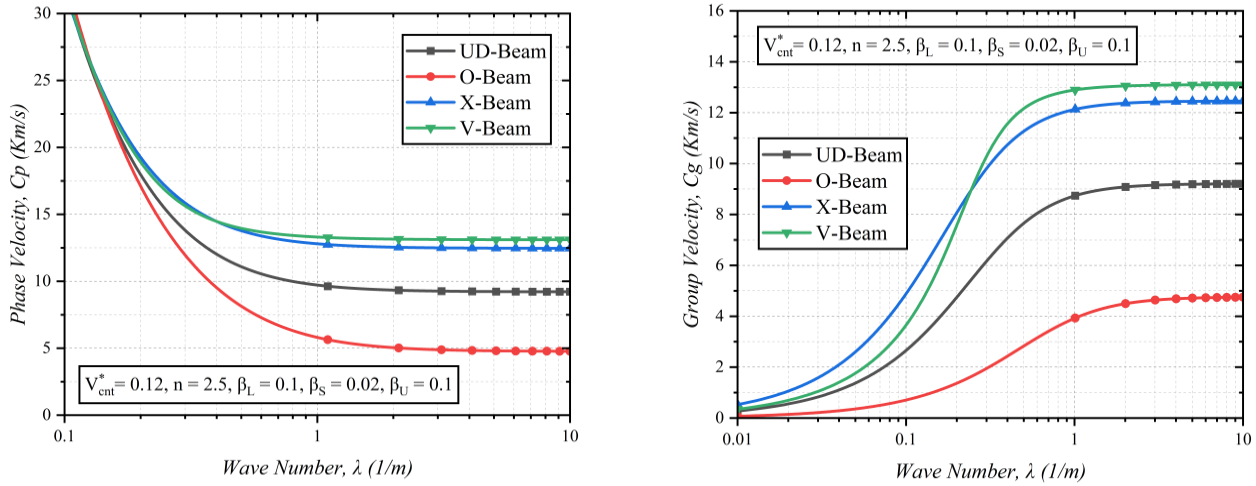

(c) Shear waves

Fig. 2 Phase (Left) and group (Right) velocities versus wavenumbers of different CNTs patterns

Fig. 5(a) indicates that both bending wave velocities of the X-beam increase slightly with increasing the degree of nonlinearity, whereas the O-beam and V-beam velocities decrease.

All pattern forms of CNTs in Fig. 5(b) exhibit constant longitudinal wave velocities with negligible change regarding the nonlinearity effect except for the V-beam, whose unsymmetric distribution of CNTs causes its

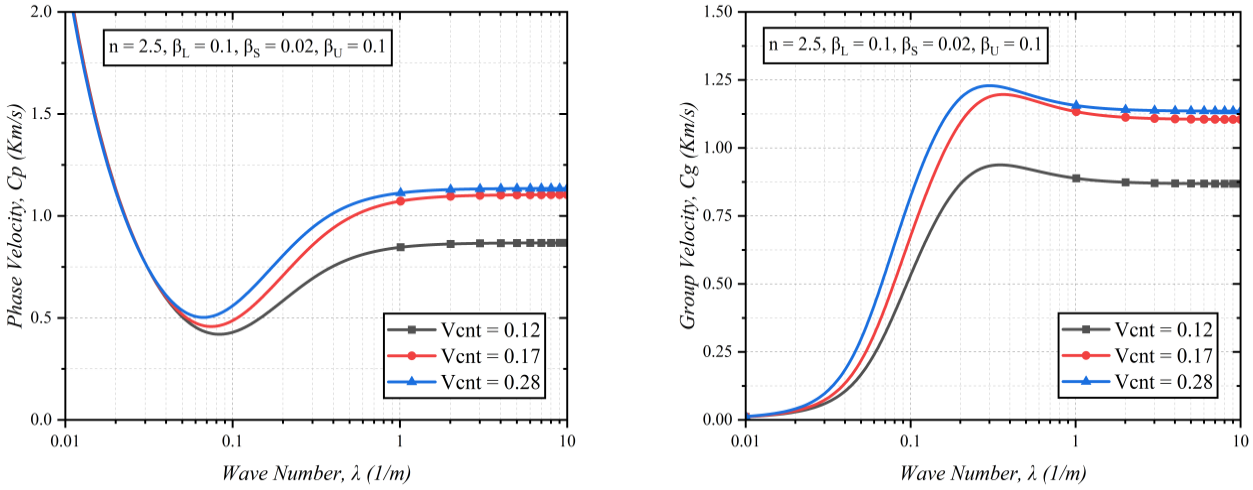

(a) Phase velocity (b) Group waves

Fig. 3 Dispersion relations of different CNTs volume fractions (X-Beam, Bending waves)

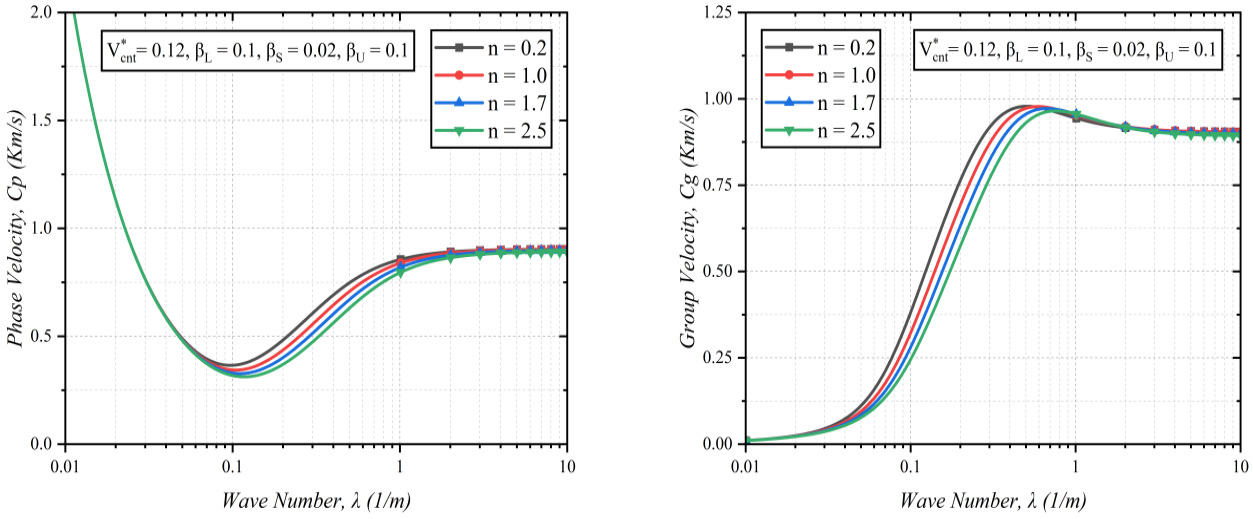

(a) Bending waves

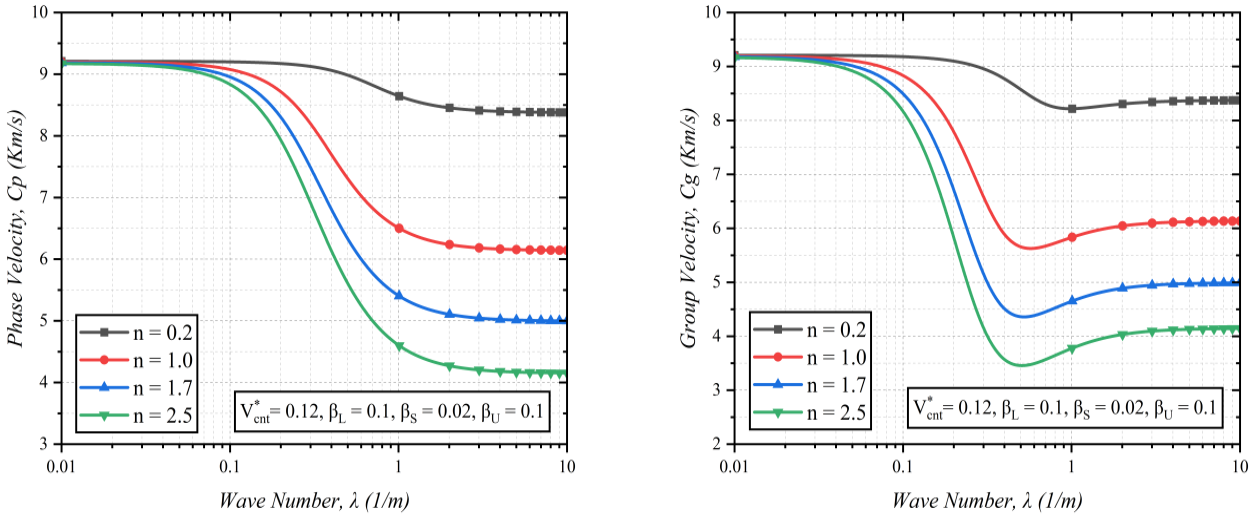

(b) Longitudinal waves

Fig. 4 Phase (Left) and group (Right) velocities versus wavenumbers of different exponent degrees

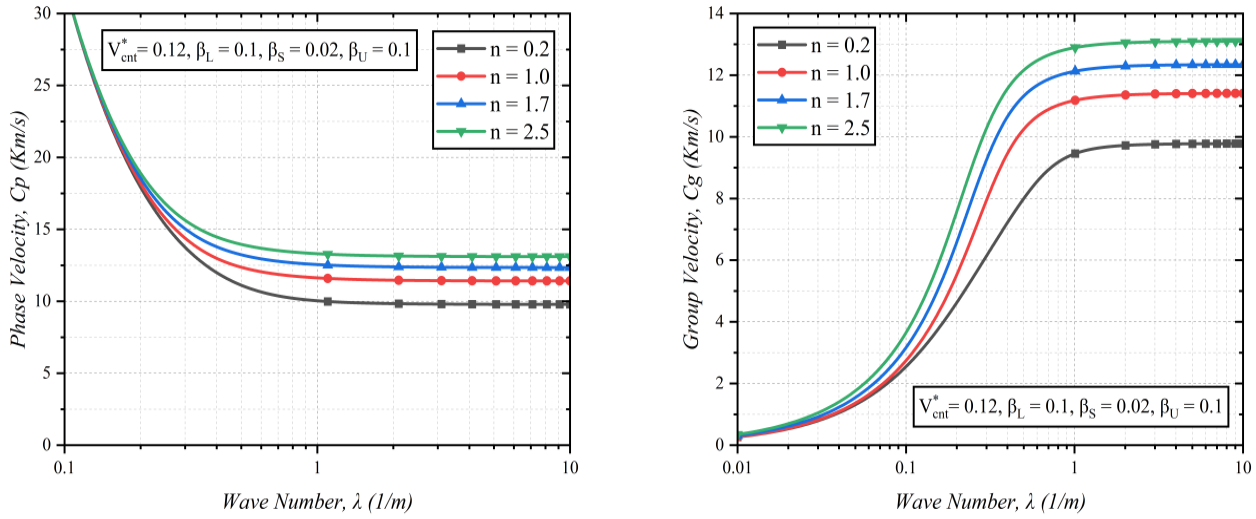

(c) Shear waves

Fig. 4 Continued-

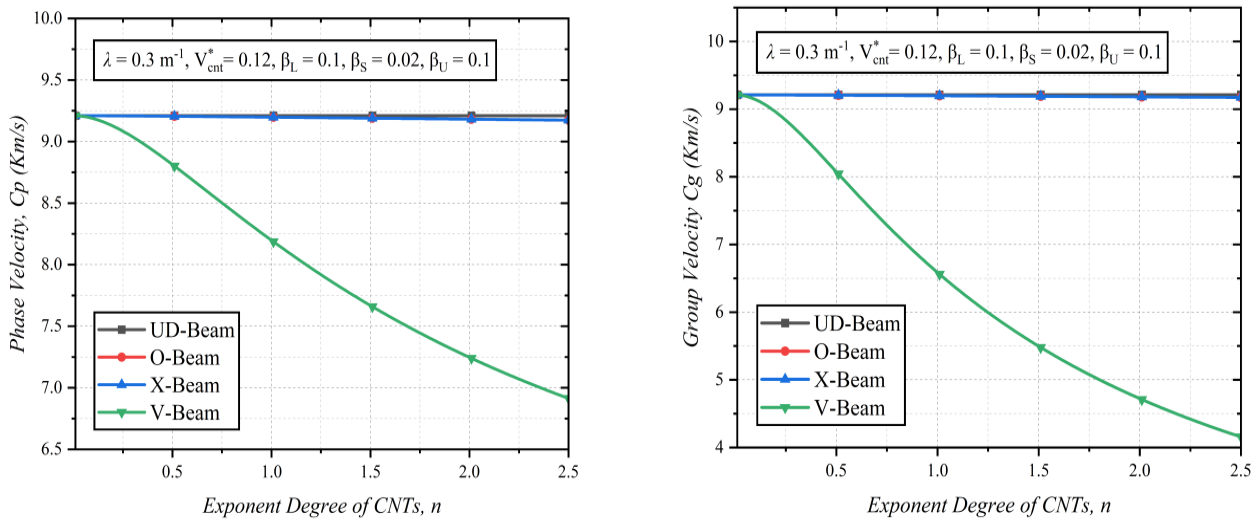

(a) Bending waves

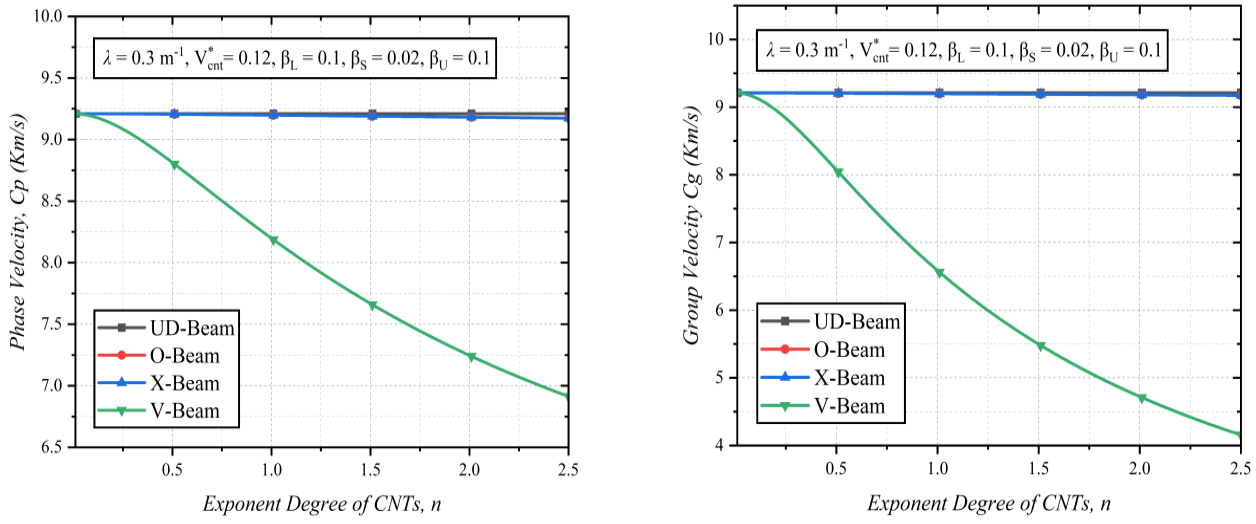

(b) Longitudinal waves

Fig. 5 Phase (Left) and group (Right) velocities versus exponent degrees of different CNTs patterns

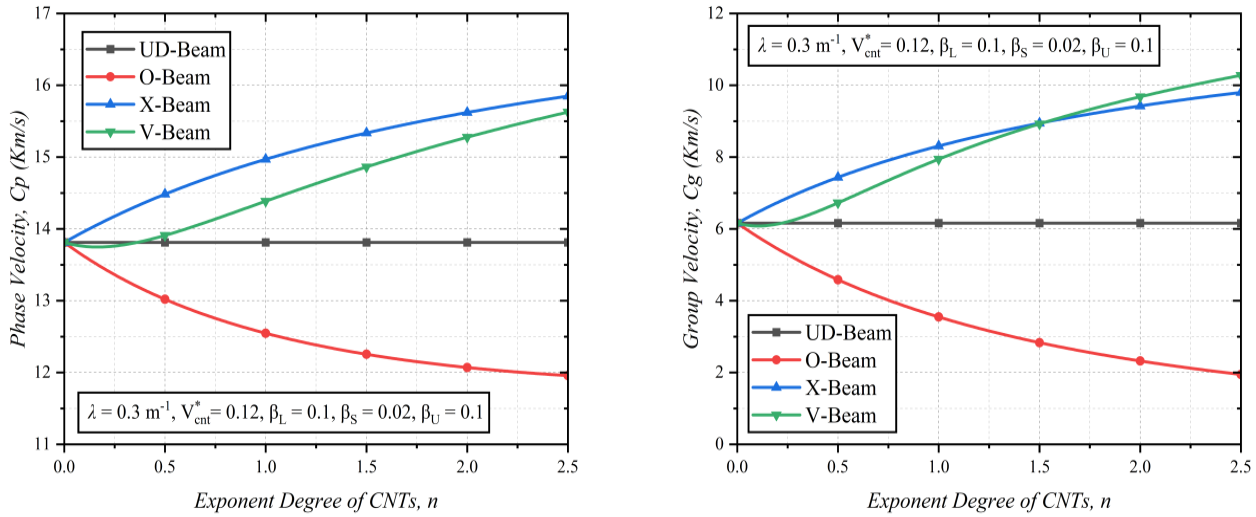

(c) Shear waves

Fig. 5 Continued-

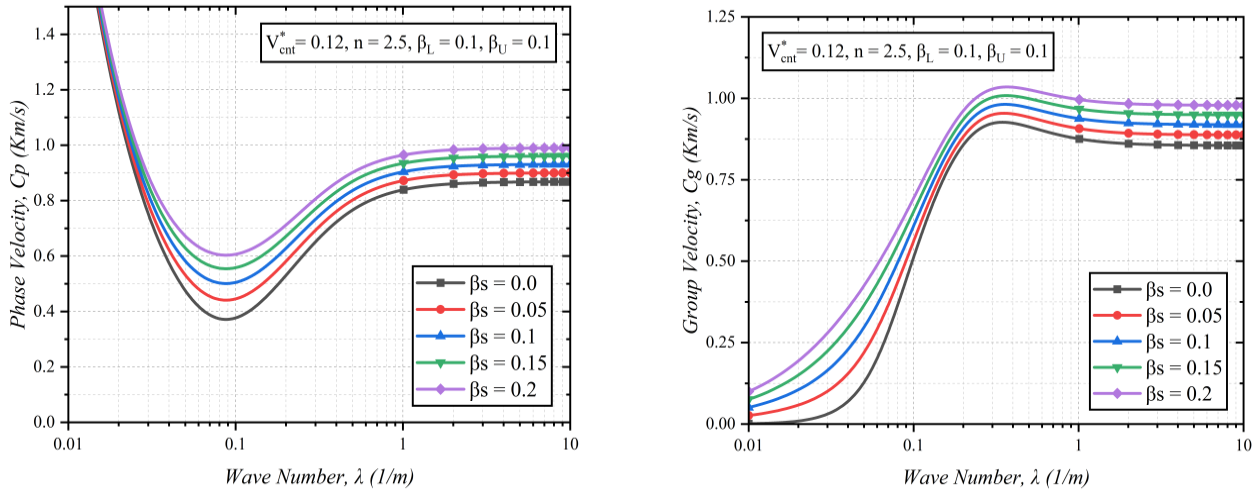

(a) Phase velocity (b) Group velocity

Fig. 6 Dispersion relations of different shear layer coefficients (X-Beam, Bending waves)

velocities to decline as values of exponent degree increase.

For shear waves, as the exponent degree increases, the phase and group velocities of X- and V- beams grow while the O-beam velocities decline, as depicted in Fig. 5(c).

All phase and group velocities of the beams approach the behavior of the UD-beam as the exponent degree decreases.

Generally, the nonlinear distribution of CNTs significantly influences the wave propagation behavior of the beams, although the extent of this impact varies based on the type of waves and the pattern forms of the CNTs. This effect arises from nonlinearity introducing a parabolic distribution of CNTs, leading to the relocation of CNTs by either concentrating or spreading them around the three linear arrangements. A higher exponent degree for the X-beam concentrates CNTs at the top and bottom edges of the cross-section, ultimately enhancing bending rigidity. In contrast, it causes CNTs to accumulate more in the center of the O-beam, reducing stiffness and rigidity. For the V-beam, the exponent degree further accentuates its asymmetric nature.

4.2.3 Effect of the Kerr foundation

The foundation affects only the wave velocities of the bending mode. All beams have nearly the same behavior regarding the foundation effect, so only the X-beam is considered a representative typical example for other beams to examine the influence of the Kerr foundation on wave propagation.

Fig. 6 illustrates the impact of the shear layer on the wave propagation of the X-beam, and it shows that as the shear layer coefficient increases, both wave velocities increase while retaining the same dispersion behavior.

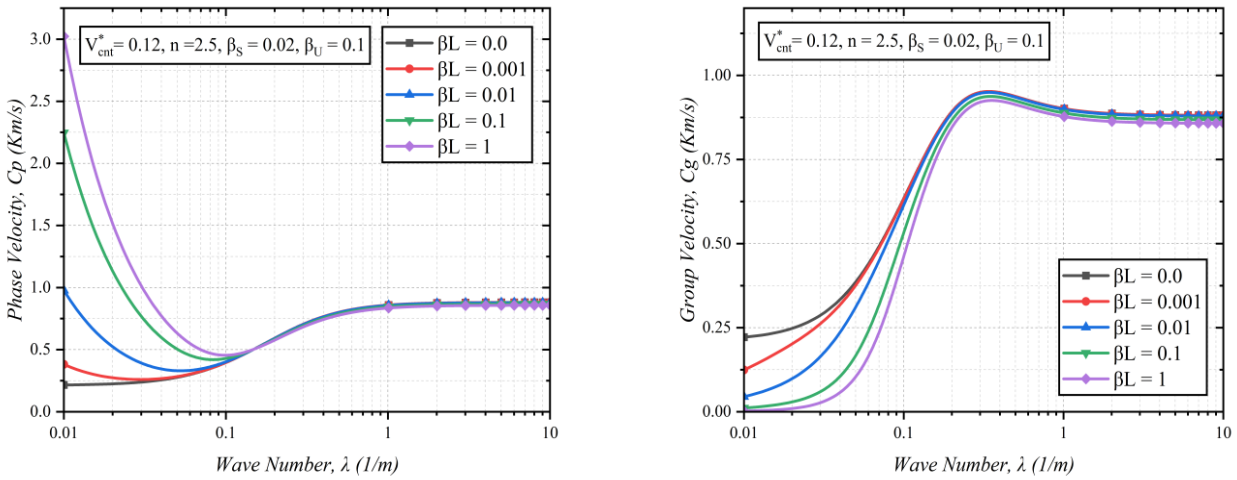

(a) Phase velocity (b) Group velocity

Fig. 7 Dispersion relations of different lower spring coefficients (X-Beam, Bending waves)

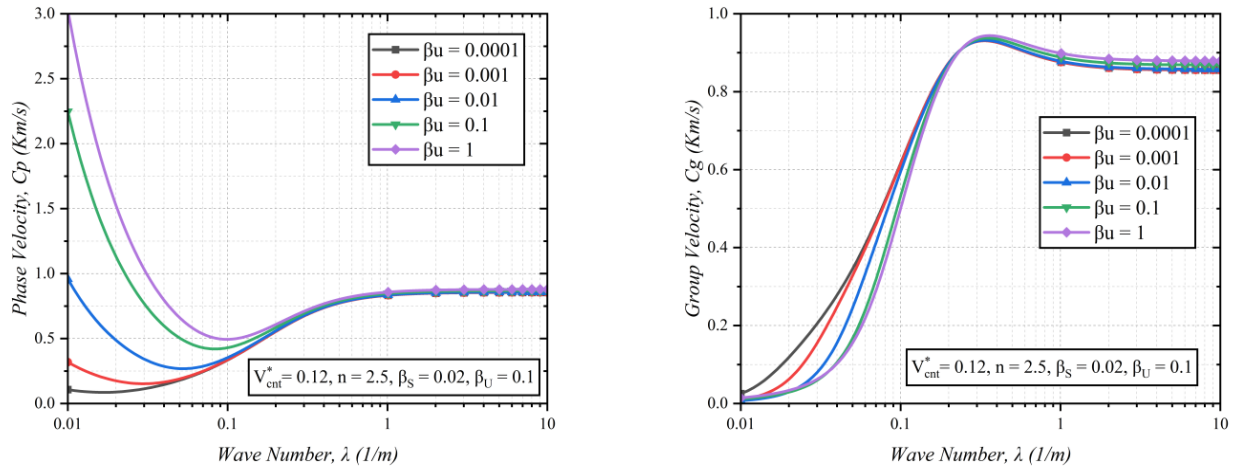

(a) Phase velocity (b) Group velocity

Fig. 8 Dispersion relations of different upper spring coefficients (X-Beam, Bending waves)

For the lower spring case, Fig. 7 shows its effect on the dispersion relations of the X-beam. The phase and group velocities are significantly impacted by the lower spring coefficient at lower wavenumbers, but this effect diminishes as the wavenumber rises. Additionally, as the coefficient of the lower spring increases, the values of phase velocities grow, contradicting the group velocities' behavior. Also worth noting is that the phase velocities change their behavior from growing to declining as the coefficient of the lower spring equals more than zero.

The impact of the upper spring on the dispersion relations of the X-beam is illustrated in Fig. 8. As in the lower spring case, at lower wavenumbers, the upper spring coefficient substantially affects both velocities; however, this effect becomes less pronounced as the wavenumber increases. In addition, as the coefficient of the upper spring grows, the values of phase velocities rise, which contradicts the behavior of group velocities. It's also important to note that the group velocities reverse their behavior when the wavenumber increases.

In the previous cases, the observed increase in wave phase velocities due to the enhanced stiffness of the foundation can be attributed to the fact that as the stiffness of the medium grows, the structural stiffness of the beams also increases.

The Various foundation types have different effects on the behavior of the propagating waves. Although the Kerr substrate is the focus of this study, other foundation types are included to compare the behavior of the current foundation with other ones. The other foundation cases include no elastic foundation, Winkler, Pasternak, and Winkler-Pasternak substrates.

Fig. 9 represents the influence of the foundation type on the dispersion relations. As can be seen in Fig. 9(a), the Kerr foundation has the third-highest phase velocities after the Winkler and Winkler-Pasternak foundations. Similarly, this confirms that the presence of a substrate or medium boosts the stiffness of the beams, thereby leading to higher phase velocities. On the other hand, the group velocities of the Kerr foundation are significantly lower compared to

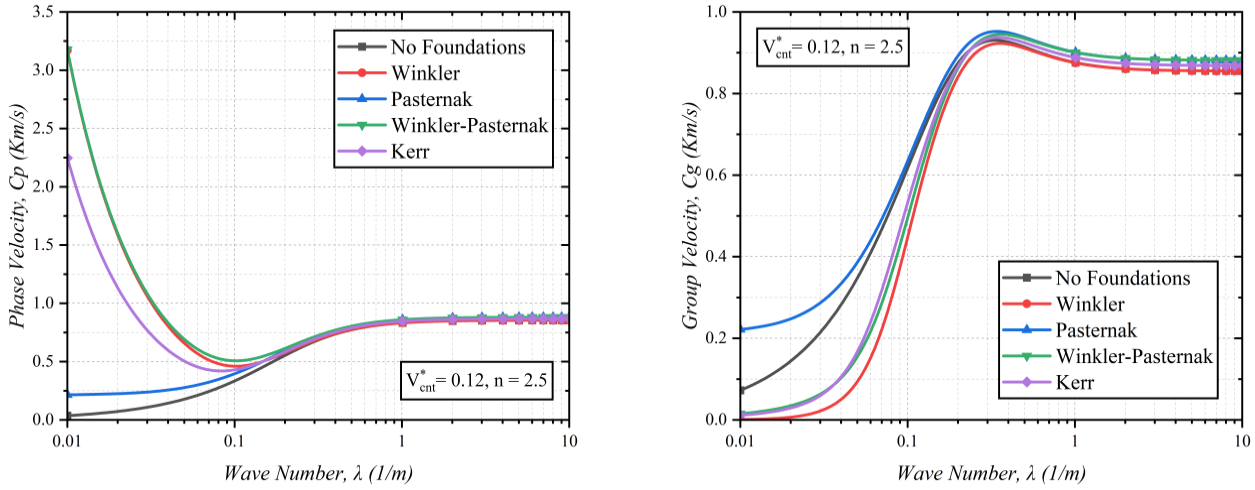

(a) Phase velocity (b) Group velocity

Fig. 9 Dispersion relations of different foundation types (X-Beam, Bending waves)

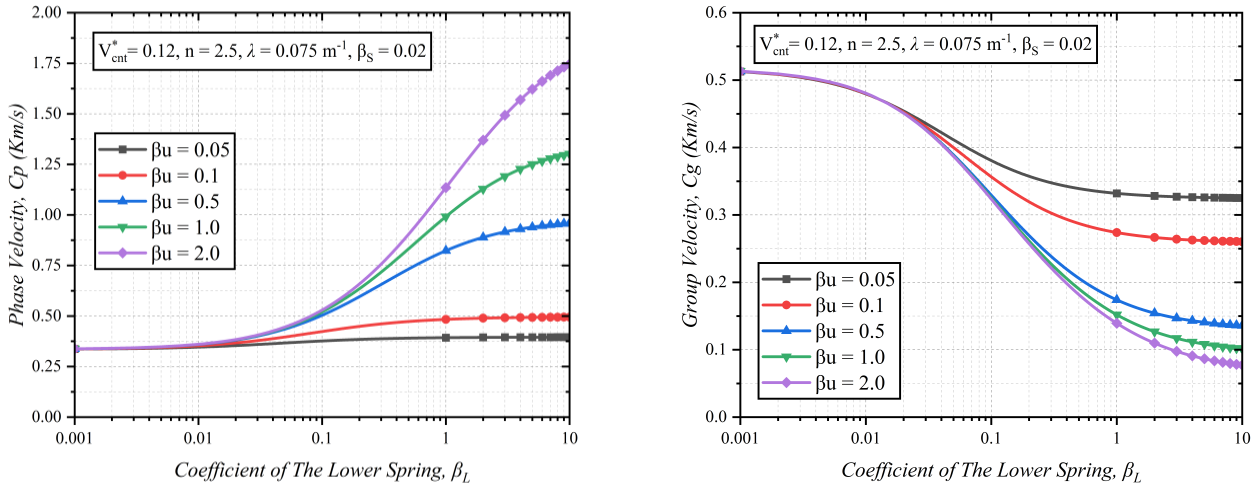

(a) Phase velocity (b) Group velocity

Fig. 10 Upper and lower springs interaction impact (X-Beam, Bending waves)

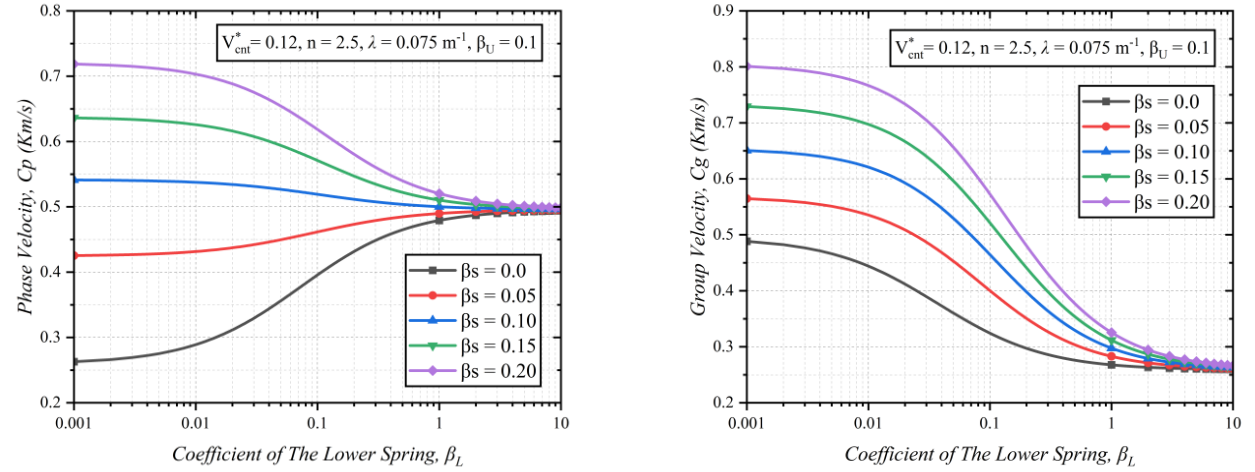

(a) Phase velocity (b) Group velocity

Fig. 11 Lower spring and shear layer interaction impact (X-Beam, Bending waves)

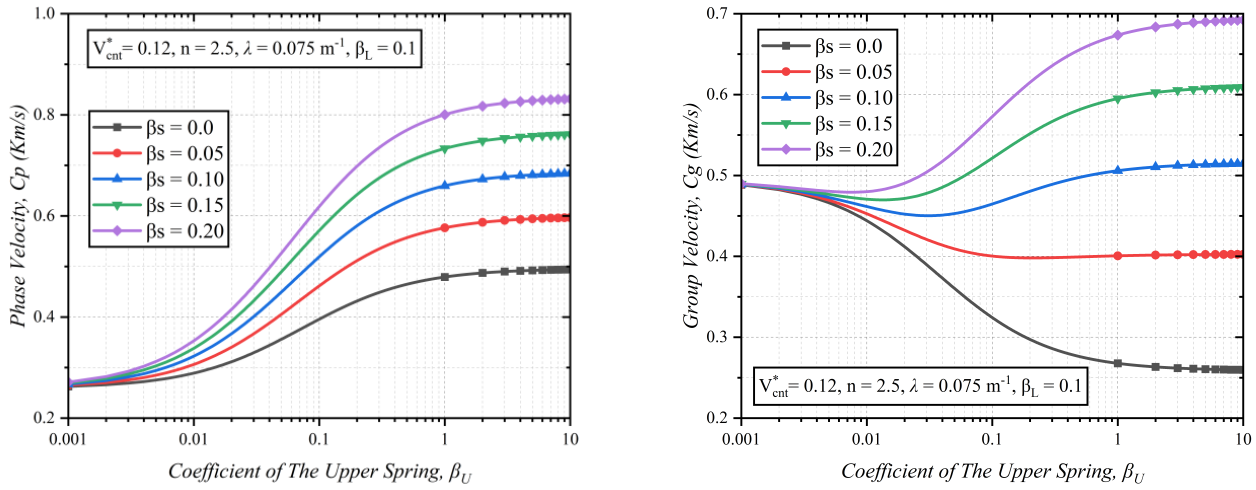

(a) Phase velocity (b) Group velocity

Fig. 12 Upper and shear layer interaction impact (X-Beam, Bending waves)

those in the no-elastic foundation and the Pasternak foundation cases, as shown in Fig. 9(b).

The interactions of the foundation springs and the shear layer with each other induce different effects on the dispersion relations. Fig. 10 depicts how the interactions between the coefficients of the upper and lower springs affect the relationship of the wave velocities while the shear layer coefficient is kept constant. Both springs enhance their impact on the propagating waves as they become stiffer, increasing the phase velocities and decreasing the group velocities.

Fig. 11 illustrates the interaction of the lower spring and shear layer on the wave velocities. Fig. 11 indicates that the shear layer tends to improve the dispersions of the wave, yet as the lower spring stiffness increases, the shear layer gradually loses its impact before becoming ineffective.

The interaction of the upper spring and shear layer on the propagating waves are shown in Fig. 12 The phase velocities are enhanced when the shear layer and upper spring become more rigid, as depicted in Fig. 12(a). Also, the group velocities reduce as the stiffness of the upper spring grows at lower values of the shear layer coefficient. However, the behavior of the group velocities flips as the shear layer's stiffness increases.

As can be concluded, as the stiffness of the two springs and the shear layer of the Kerr foundation varies, its behavior changes and approaches that of other substrate types, leading to these intriguing results.

5. Conclusions

This paper investigated the wave propagation behavior of composite beams reinforced with nonlinear distribution patterns of FG-CNTs supported by Kerr substrate and utilizing an improved integral FSDT with three variables. The bending, longitudinal, and shear propagating waves of FG-CNTRC were discussed in the analysis. Four distinct configurations of SWCNTs were employed in the study. The governing equations were derived and solved using the wave propagation solution and Hamilton's principle. The parametric study examined how the volume fractions and dispersion patterns of the CNTs affected the wave propagation responses. Furthermore, the study examined the impact of the Kerr foundation and the degree of the nonlinear model on the behavior of the waves.

Numerical analysis revealed the following findings:

- The implementation of FSDT simplifies the derivation process without sacrificing accuracy. Also, incorporating an integral form allows for precise shear rotations while introducing a novel corrective function enables a better distribution of shear stresses and strains. Hence, the fundamental frequency results from this improved integral FSDT theory closely match those obtained from HSDT.
- The arrangements of CNTs manipulate the axial, flexural, and shear rigidities of the FG-CNTRC beams ultimately affecting the dispersion relations.
- Reinforcing the beams by providing more volume fractions of CNTs improves the stiffness of the beams and results in higher propagating velocities.
- The nonlinear distributions of CNTs significantly impact the wave propagation of the FG-CNTRC beams, depending on the wave type and pattern forms of CNTs. This is due to the parabolic distribution, which relocates the CNTs by either concentrating or spreading them, thereby altering the stiffness of the beams.
- Supporting the FG-CNTRC beams with a foundation boosts their stiffness, leading to higher phase velocities. Hence, as the stiffness of the foundation grows, the phase velocities increase. Notably, only the bending waves are affected by the presence of the foundation.
- The interactions of the foundation two springs and the shear layer induce different effects on the dispersion relations. These results arise from the alterations in the stiffness of the Kerr foundation's components, causing its behavior to resemble that of other substrate types.

Finally, the current improved model can be employed in future work to examine the wave propagation response of other materials as used in (Daouadji and Hadji 2015, Yaylaci 2016, Ghorbanpour-Arani *et al.* 2016, 2017, Ghorbanpour *et al.* 2017, Akbas 2018a, b, Fenjan *et al.* 2020, Karami and Karami 2019, Madenci 2019, Hadji 2020, Rachedi *et al.* 2020, Merzoug *et al.* 2020, Yaylaci and Avcar 2020, Ahmed *et al.* 2019, Mehar and Panda 2019, Timesli 2020, Madenci and Özütok 2020, Yaylaci *et al.* 2021,Öner *et al.* 2022, Yaylaci 2022, Yaylaci *et al.* 2022c, d, e, Turan *et al.* 2022, Ding *et al.* 2022, Abadi 2023, Behshad *et al.* 2023, Abad *et al.* 2023, Yaylaci *et al.* 2023abcd, Xu and She 2023, Rossi and Spinella 2023, Ghandourah *et al*. 2023, Ozdemir and Yaylaci 2023, Song *et al.* 2024, Mohamed *et al.* 2024).

Acknowledgments

The authors would like to acknowledge the support provided by the Interdisciplinary Research Center for Construction & Building Materials (IRC-CBM) at King Fahd University of Petroleum & Minerals (KFUPM), Saudi Arabia, for funding this work through Project No. INCB2209. The support provided by the Department of Civil & Environmental Engineering, KFUPM, Saudi Arabia, is also greatly acknowledged.

References

Adıyaman, G., Öner, E., Yaylacı, M. and Birinci, A. (2023), "A study on the contact problem of a layer consisting of functionally graded material (FGM) in the presence of body force", *J. Mech. Mater. Struct.*, **18**(1), 125-141. https://doi.org/10.2140/jomms.2023.18.125.

Abad, F., Rouzegar, J. and Lotfian, S. (2023), "Application of the exact spectral element method in the analysis of the smart functionally graded plate", *Steel Compos. Struct.*, **47**(2), 297-313. https://doi.org/10.12989/scs.2023.47.2.297.

Abadi, M.T. (2023), "Analysis of elastic wave propagation in long beam using Fourier transformation", *Struct. Eng Mech.*, **87**(2), 165-172. https://doi.org/10.12989/sem.2023.87.2.165.

Ahmed, R.A., Fenjan, R.M. and Faleh, N.M. (2019), "Analyzing post-buckling behavior of continuously graded FG nanobeams with geometrical imperfections", *Geomech. Eng.*, **17**(2), 175-180. https://doi.org/10.12989/gae.2019.17.2.175.

Ajayan, P.M. and Tour, J.M. (2007), "Nanotube composites", *Nature*, **447**(7148), 1066-1068. https://doi.org/10.1038/4471066a.

Akbas, S.D. (2015), "Wave propagation of a functionally graded beam in thermal environments", *Steel Compos. Struct*., **19**(6), 1421-1447. https://doi.org/10.12989/scs.2015.19.6.1421.

Akbas, S.D. (2018a), "Geometrically nonlinear analysis of a laminated composite beam", *Struct. Eng. Mech.*, **66**(1), 27-36. https://doi.org/10.12989/sem.2018.66.1.027.

Akbas, S.D. (2018b), "Thermal post-buckling analysis of a laminated composite beam", *Struct. Eng. Mech.*, **67**(4), 337-346. https://doi.org/10.12989/sem.2018.67.4.337.

Al-Basyouni, K.S., Ghandourah, E., Mostafa, H.M. and Algarni, A. (2020), "Effect of the rotation on the thermal stress wave propagation in non-homogeneous viscoelastic body", *Geomech. Eng.*, **21**(1), 1-9. https://doi.org/10.12989/gae.2020.21.1.001.

Alibeigloo, A. (2013), "Static analysis of functionally graded carbon nanotube-reinforced composite plate embedded in piezoelectric layers by using theory of elasticity", *Compos Struct*., **95**, 612-622. https://doi.org/10.1016/J.COMPSTRUCT.2012.08.018.

Al-Osta, M.A. (2022), "Wave propagation investigation of a porous sandwich FG plate under hygrothermal environments via a new first-order shear deformation theory", *Steel Compos. Struct.*, **43**(1), 117-127. https://doi.org/10.12989/scs.2022.43.1.117.

Alsubaie, A.M., Alfaqih, I., Al-Osta, M.A., Tounsi, A., Chikh, A., Mudhaffar, I.M. and Tahir, S. (2023), "Porosity-dependent vibration investigation of functionally graded carbon nanotube-reinforced composite beam", *Comput. Concrete*, **32**(1), 75-85. https://doi.org/10.12989/cac.2023.32.1.075.

Arani, A.G., Haghparast, E. and Arani, A.H.G. (2014), "Size-dependent vibration of double-bonded carbon nanotube-reinforced composite microtubes conveying fluid under longitudinal magnetic field", *Polymer Compos.*, **37**(5), 1375-1383. https://doi.org/10.1002/pc.23306.

Arani, A.H.G., Abdollahian, M. and Arani, A.G. (2020), "Nonlinear dynamic analysis of temperature-dependent functionally graded magnetostrictive sandwich nanobeams using different beam theories", *J. Braz. Soc. Mech. Sci. Eng.*, **42**(314). https://doi.org/10.1007/s40430-020-02400-8.

Avcar, M. (2019), "Free vibration of imperfect sigmoid and power law functionally graded beams", *Steel Compos. Struct.*, **30**(6), 603-615. https://doi.org/10.12989/scs.2019.30.6.603.

Behshad, A., Shokravi, M., Alavijeh, A.S. and Karami, H. (2023), "Elastic wave propagation analysis in sandwich nanoplate assuming size effects", *Steel Compos. Struct.*, **47**(1), 71-77. https://doi.org/10.12989/scs.2023.47.1.071.

Bharti, I. and Gupta, N. (2013), "Novel applications of functionally graded nano, optoelectronic and thermoelectric materials", *Int. J. Mater. Mech. Manufact.*, **1**(3), 221-224. https://doi.org/10.7763/IJMMM.2013.V1.47.

Birgani, Y.A., Arani, A.G. and Maraghi, Z.K. (2024), "Nonlocal buckling analysis of five-layer laminated nanocomposites on kerr foundation: A refined zigzag theory approach", *J. Sandw. Struct. Mater.*, **26**(8), 1436-1465. https://doi.org/10.1177/10996362241280020.

Bosi, S., Fabbro, A., Ballerini, L. and Prato, M. (2012), "Carbon nanotubes: A promise for nerve tissue engineering?", *Nanotechnol. Rev*., **2**, 47-57. https://doi.org/10.1515/ntrev-2012-0067.

Chaikittiratana, A. and Wattanasakulpong, N. (2022), "Dynamic loadings induced vibration of third order shear deformable FG-CNTRC beams: Gram-schmidt-ritz method", *Adv. Appl. Math. Mech.*, **14**, 816-841. https://doi.org/10.4208/AAMM.OA-2020-0177.

Chalak, H.D., Zenkour, A.M. and Garg, A. (2023), "Free vibration and modal stress analysis of FG-CNTRC beams under hygrothermal conditions using zigzag theory", *Mech. Based Des. Struc.*, **51**, 4709-4730. https://doi.org/10.1080/15397734.2021.1977659.

Chen, C.S., Fung, C.P., Wang, H. and Chen, W.R. (2022), "Dynamic response of functionally graded carbon nanotube-reinforced hybrid composite plates", *J. Appl. Comput. Mech*., **8**, 182–95. https://doi.org/10.22055/JACM.2021.37884.3108.

Cho, J.R. (2022), "Nonlinear bending analysis of functionally graded CNT-reinforced composite plates", *Steel Compos. Struct*., **42**(1), 23-32. https://doi.org/10.12989/scs.2022.42.1.023.

Dai, T., Yang, Y., Dai, H.L., Tang, H. and Lin, Z.Y. (2019), "Hygrothermal mechanical behaviors of a porous FG-CRC annular plate with variable thickness considering aggregation of CNTs", *Compos. Struct.*, **215**, 198-213. https://doi.org/10.1016/j.compstruct.2019.02.061.

Daouadji, T.H. and Hadji, L. (2015), "Analytical solution of nonlinear cylindrical bending for functionally graded plates", *Geomech. Eng.*, **9**(5), 631-644. https://doi.org/10.12989/gae.2015.9.5.631.

Ding, H.X., Liu, H.B., She, G.L. and Wu, F. (2023), "Wave propagation of FG-CNTRC plates in thermal environment using the high-order shear deformation plate theory", *Comput. Concrete*, **32**(2), 207-215. https://doi.org/10.12989/cac.2023.32.2.207.

Ding, H.X., Zhang, Y.W. and She, G.L. (2022), "On the resonance problems in FG-GPLRC beams with different boundary conditions resting on elastic foundations", *Comput. Concrete*, **30**(6), 433-443. https://doi.org/10.12989/cac.2022.30.6.433.

Dresselhaus, M.S., Dresselhaus, G. and Avouris, P. (2001), "Carbon nanotubes: Synthesis, structure, properties, and applications", *Springer*. https://doi.org/10.1007/3-540-39947-X.

Ebrahimi, F. and Rostami, P. (2018a), "Propagation of elastic waves in thermally affected embedded carbon-nanotube-reinforced composite beams via various shear deformation plate theories", *Struct. Eng. Mech*., **66**(4), 495-504. https://doi.org/10.12989/sem.2018.66.4.495.

Ebrahimi, F. and Rostami, P. (2018b), "Wave propagation analysis of carbon nanotube reinforced composite beams", *Eur. Phys. J. Plus.,* **133**, 285. https://doi.org/10.1140/epjp/i2018-12069-y.

Ebrahimi, F., Seyfi, A. and Dabbagh, A. (2021), "The effects of thermal loadings on wave propagation analysis of multi-scale hybrid composite beams", *Waves in Random and Complex Media*, **34**(4), 2342-2365. https://doi.org/10.1080/17455030.2021.1956015.

Fenjan, R.M., Faleh, N.M. and Ahmed, R.A. (2020), "Geometrical imperfection and thermal effects on nonlinear stability of microbeams made of graphene-reinforced nano-composites", *Adv. Nano Res.*, **9**(3), 147-156. https://doi.org/10.12989/anr.2020.9.3.147.

Gan, L.L., Xu, J.Q. and She, G.L. (2023), "Wave propagation of graphene platelets reinforced metal foams circular plates", *Struct. Eng. Mech*., **85**(5), 645-654. https://doi.org/10.12989/sem.2023.85.5.645.

Gawah, Q., Bourada, F., Al-Osta, M.A., Tahir, S.I., Tounsi, A. and Yaylacl, M. (2024), "An improved first-order shear Deformation theory for wave propagation analysis in FG-CNTRC beams resting on a viscoelastic substrate", *Int. J. Struct. Stab. Dyn.*, 2550010. https://doi.org/10.1142/S0219455425500105.

Ghandourah, E., Hussain, M., Khadimallah, M.A., Alazwari, M., Ali, M.R. and Hefni, M.A. (2023), "Validity assessment of aspect ratios based on Timoshenko-beam model: Structural design", *Comput. Concrete*, **31**(1), 1-7. https://doi.org/10.12989/cac.2023.31.1.001.

Ghorbanpour, A., Jamali, M., Ghorbanpour-Arani A.H., Kolahchi, R. and Mosayyebi, M. (2017), "Electro-magneto wave propagation analysis of viscoelastic sandwich nanoplates considering surface effects", *Proceedings of the Institution of Mechanical Engineers, Part C: J. Mechanical Engineering Science*. **231**(2), 387-403. https://doi.org/10.1177/0954406215627830.

Ghorbanpour-Arani, A.H., Rastgoo, A., Hafizi Bidgoli, A., Kolahchi, R. and Ghorbanpour Arani, A. (2017), "Wave propagation of coupled double-DWBNNTs conveying fluid-systems using different nonlocal surface piezoelasticity theories", *Mech. Adv. Mater. Struct*., **24**(14), 1159-1179. https://doi.org/10.1080/15376494.2016.1227488.

Ghorbanpour-Arani, A.H., Rastgoo, A., Sharafi, M.M., Kolahchi, R. and Ghorbanpour-Arani, A.H. (2016), "Nonlocal viscoelasticity based vibration of double viscoelastic piezoelectric nanobeam systems", *Meccanica*, **51**, 25-40. https://doi.org/10.1007/s11012-014-9991-0.

Gopalakrishnan, S. and Narendar, S. (2013), "Wave Propagation in 2D-Nanostructures. In: Wave Propagation in Nanostructures. NanoScience and Technology", *Springer, Cham*. https://doi.org/10.1007/978-3-319-01032-8_10.

Hadji, L. (2020), "Influence of the distribution shape of porosity on the bending of FGM beam using a new higher order shear deformation model", *Smart Struct. Syst.*, **26**(2), 253-262. https://doi.org/10.12989/sss.2020.26.2.253.

Haghparast, E., Arani, A.A.G. and Arani, A.G. (2020), "Effect of fluid–structure interaction on vibration of moving sandwich plate with balsa wood core and nanocomposite face sheets", *Int. J. Appl. Mech.*, **12**(7), 2050078. https://doi.org/10.1142/s1758825120500787.

Hao, Y. and Li, F. (2023), "Wave propagation characteristics of piezoelectric FG-CNTRC plates", *Proceedings of the 17th Symposium on Piezoelectricity, Acoustic Waves, and Device Applications (SPAWDA)*, Chengdu, China. https://doi.org/10.1109/SPAWDA60286.2023.10412329.

Hosseini, M., Chahargonbadizade, P. and Mofidi, M. (2023), "Wave propagation analysis of carbon nanotubes reinforced composite plates", *Struct. Eng. Mech.*, **88**(4), 335-354. https://doi.org/10.12989/sem.2023.88.4.335.

Houalef, I.E., Bensaid, I., Saimi, A. and Cheikh, A. (2023), "Free vibration analysis of functionally graded carbon nanotube-reinforced higher order refined composite beams using differential quadrature finite element method", *Eur. J. Comput. Mech.,* **31**(4), 505-538. https://doi.org/10.13052/ejcm2642-2085.3143.

Iijima, S. (1991), 'Helical microtubules of graphitic carbon", *Nature*., **6348**, 56-58. https://doi.org/10.1038/354056a0.

Janghorban, M. and Nami, M.R. (2017), "Wave propagation in functionally graded nanocomposites reinforced with carbon nanotubes based on second-order shear deformation theory", *Mech. Adv. Mater Struct*., **24**, 458-468. https://doi.org/10.1080/15376494.2016.1142028.

Jenabi, J., Nezamabadi, A.R. and Khorramabadi, M.K. (2024), "Nonlinear bending of multilayer functionally graded graphene-reinforced skew microplates under mechanical and thermal loads using FSDT and MCST: A study in large deformation", *Struct. Eng. Mech.*, **90**(3), 219-232. https://doi.org/10.12989/sem.2024.90.3.219.

Karami, B. and Karami, S. (2019), "Buckling analysis of nanoplate-type temperature-dependent heterogeneous materials", *Adv. Nano Res.*, **7**(1), 51-61. https://doi.org/10.12989/anr.2019.7.1.051.

Kerr, A.D. (1965), "A study of a new foundation model", *Acta Mechanica*, **1**, 135-147. https://doi.org/10.1007/BF01174308.

Kim Y. and Kuljanishvili I. (2023), "Recent advances in carbon nanotube patterning technologies for device applications", *Front. Carbon*, **2**. https://doi.org/10.3389/frcrb.2023.1288912.

Kong, J., Franklin, N.R., Zhou, C., Chapline, M.G., Peng, S., Cho, K. and Dai, H. (2000), "Nanotube molecular wires as chemical sensors", *Science*, **287**(5453), 622-625. https://doi.org/10.1126/science.287.5453.622.

Kumar, M. and Sarangi, S.K. (2022), "Bending and vibration study of carbon nanotubes reinforced functionally graded smart composite beams", *Eng. Res. Express*., **4**, 025043. https://doi.org/10.1088/2631-8695/AC76A0.

Liu, M., Bi, S., Shao, S. and Babaei, H. (2023), "Nonlinear vibration of FG-CNTRC curved pipes with temperature-dependent properties", *Steel Compos. Struct*., **46**(4), 553-563. https://doi.org/10.12989/scs.2023.46.4.553.

Long, C., Wang, D. and Xiang, H.B. (2023), "Static and dynamic bending of ball reinforced by CNTs considering agglomeration effect", *Steel Compos. Struct.*, **48**(4), 419-428. https://doi.org/10.12989/scs.2023.48.4.419.

Madenci, E. (2019), "A refined functional and mixed formulation to static analyses of fgm beams", *Struct. Eng. Mech.*, **69**(4),

427-437. https://doi.org/10.12989/sem.2019.69.4.427.
Madenci, E. and Özütok, A. (2020), "Variational approximate for high order bending analysis of laminated composite plates", *Struct. Eng. Mech.*, **73**(1), 97-108. https://doi.org/10.12989/sem.2020.73.1.097,
Mehar, K. and Panda, S.K. (2019), "Multiscale modeling approach for thermal buckling analysis of nanocomposite curved structure", *Adv. Nano Res.*, **7**(3), 181-190. https://doi.org/10.12989/anr.2019.7.3.181.
Merzoug, M., Bourada, M., Sekkal, M., Ali Chaibdra, A., Belmokhtar, C., Benyoucef, S. and Benachour, A. (2020), "2D and quasi 3D computational models for thermoelastic bending of FG beams on variable elastic foundation: Effect of the micromechanical models", *Geomech. Eng.*, **22**(4), 361-374. https://doi.org/10.12989/gae.2020.22.4.361.
Mohamed, S.A., Assie, A.E., Eltaher, M.A., Abo-bakr, R.M. and Mohamed, N. (2024), "Nonlinear postbuckling and snap-through instability of movable simply supported BDFG porous plates rested on elastic foundations", *Mech. Based Des. Struc*., 1-28. https://doi.org/10.1080/15397734.2024.2328339.
Moniruzzaman, M. and Winey, K.I. (2006), "Polymer nanocomposites containing carbon nanotubes", *Macromolecules*, **39**(16), 5194-5205. https://doi.org/10.1021/ma060733p.
Niino, M. and Maeda, S. (1990), "Recent development status of functionally gradient materials", *ISIJ Int*., **30**, 699-703. https://doi.org/10.2355/ISIJINTERNATIONAL.30.699.
Öner, E., Bahar , B.Ş., Yaylacı, E.U., Adıyaman, G., Yaylacı, M. and Birinci, A. (2022), "On the plane receding contact between two functionally graded layers using computational, finite element and artificial neural network methods", *ZAMM – J. Appl. Math. Mech. / Zeitschrift für Angewandte Mathematik und Mechanik*., **102**(2), 202100287. https://doi.org/10.1002/zamm.202100287.
Ong, O.Z.S., Ghayesh, M.H. and Losic, D. (2023), "Vibrations of porous functionally graded CNT reinforced viscoelastic beams connected via a viscoelastic layer", *Int. J. Eng. Sci*., **191**, 103917. https://doi.org/10.1016/J.IJENGSCI.2023.103917.
Ozbey, M.B., Cuma, Y.C., Deneme, I.O. and Calim, F.F. (2024), "Free and forced vibration analysis of FG-CNTRC viscoelastic plate using high shear deformation theory", *Adv. Nano Res.,* **16**(4), 413-426. https://doi.org/10.12989/anr.2024.16.4.413.
Ozdemir, M.E. and Yaylaci, M. (2023), "Research of the impact of material and flow properties on fluid-structure interaction in cage systems", *Wind Struct.*, **36**(1), 31-40. https://doi.org/10.12989/was.2023.36.1.031.
Rachedi, M.A., Benyoucef, S., Bouhadra, A., Bachir Bouiadjra, R., Sekkal, M. and Benachour, A. (2020), "Impact of the homogenization models on the thermoelastic response of FG plates on variable elastic foundation", *Geomech. Eng.*, **22**(1), 65-80. https://doi.org/10.12989/gae.2020.22.1.065.
Rossi, P.P. and Spinella, N. (2023), "Extension of theoretical approaches for the shear strength of reinforced concrete beams with corroded stirrups", *Comput. Concrete*, **31**(1), 33-52. https://doi.org/10.12989/cac.2023.31.1.033.
Ruoff, R.S. and Lorents, D.C. (1995), "Mechanical and thermal properties of carbon nanotubes", *Carbon*, **33**(7), 925-930. https://doi.org/10.1016/0008-6223(95)00021-5.
Sahoo, S., Parida, S.P. and Jena, P.C. (2023), "Dynamic response of a laminated hybrid composite cantilever beam with multiple cracks & moving mass", *Struct. Eng. Mech*., **87**(6), 529-540. https://doi.org/10.12989/sem.2023.87.6.529.
Saito, R., Dresselhaus, G. and Dresselhaus, M.S. (1998), "Physical Properties of Carbon Nanotubes", *Imperial College Press*. https://doi.org/10.1142/p080
Selmi, A. (2020), "Exact solution for nonlinear vibration of clamped-clamped functionally graded buckled beam", *Smart Struct. Syst.,* **26**(3), 361-371. https://doi.org/10.12989/sss.2020.26.3.361.
Seyfi, A., Teimouri, A., Dimitri, R. and Tornabene, F. (2022), "Dispersion of elastic waves in functionally graded CNTs-reinforced composite beams", *Appl. Sci*., **12**, 3852. https://doi.org/10.3390/APP12083852.
Shen, H.S. (2009), "Nonlinear bending of functionally graded carbon nanotube-reinforced composite plates in thermal environments", *Compos. Struct.*, **91**(1), 9-19. https://doi.org/10.1016/j.compstruct.2009.04.026.
Shen, H.S., Huang, X.H. and Yang, J. (2020), "Nonlinear bending of temperature-dependent FG-CNTRC laminated plates with negative Poisson's ratio", *Mech. Adv Mater. Struct.*, **27**, 1141-53. https://doi.org/10.1080/15376494.2020.1716412.
Singh, S.D. and Sahoo, R. (2021), "Analytical solution for static and free vibration analysis of functionally graded CNT-reinforced sandwich plates", *Arch. Appl. Mech*., **91**, 3819-3834. https://doi.org/10.1007/s00419-021-01979-1.
Song, J.P., She, G.L. and Eltaher, M.A. (2024), "Nonlinear aero-thermo-elastic flutter analysis of stiffened graphene platelets reinforced metal foams plates with initial geometric imperfection", *Aerosp. Sci. Technol.*, **147**, 109050. https://doi.org/10.1016/j.ast.2024.109050.
Soni, S.K., Thomas, B., Swain, A. and Swain, T. (2022), "Functionally graded carbon nanotubes reinforced composite structures: An extensive review", *Compos. Struct.*, **299**. https://doi.org/10.1016/j.compstruct.2022.116075.
Tagrara, S.H., Benachour, A., Bouiadjra, M.B. and Tounsi, A. (2015), "On bending, buckling and vibration responses of functionally graded carbon nanotube-reinforced composite beams", *Steel Compos. Struct.*, **19**(5), 1259-1277. https://doi.org/10.12989/scs.2015.19.5.1259.
Tans, S.J., Devoret, M.H., Dai, H., Thess, A., Smalley, R.E., Geerligs, L.J. and Dekker, C. (1997), "Individual single-wall carbon nanotubes as quantum wires", *Nature*, **386**(6624), 474-477. https://doi.org/10.1038/386474a0.
Thostenson, E.T., Ren, Z. and Chou, T.W. (2001), "Advances in the science and technology of carbon nanotubes and their composites: A review", *Compos. Sci. Technol.*, **61**(13), 1899-1912. https://doi.org/10.1016/S0266-3538(01)00094-X.
Timesli, A. (2020), "Prediction of the critical buckling load of SWCNT reinforced concrete cylindrical shell embedded in an elastic foundation", *Comput. Concrete*, **26**(1), 53-62. https://doi.org/10.12989/cac.2020.26.1.053.
Turan, M., Yaylaci, E.U. and Yaylaci, M. (2022), "Free vibration and buckling of functionally graded porous beams using analytical, finite element, and artificial neural network methods", *Arch. Appl. Mech.*, **93**(4), 1351-1372. https://doi.org/10.1007/s00419-022-02332-w.
Wattanasakulpong, N. and Ungbhakorn, V. (2013), "Analytical solutions for bending, buckling and vibration responses of carbon nanotube-reinforced composite beams resting on elastic foundation", *Comput. Mater. Sci*., **71**, 201-208. https://doi.org/10.1016/j.commatsci.2013.01.028.
Wong, E.W., Sheehan, P.E. and Lieber, C.M. (1997), "Nanobeam mechanics: Elasticity, strength, and toughness of nanorods and nanotubes", *Science*, **277**(5334), 1971-1975. https://doi.org/10.1126/science.277.5334.1971.
Wu, F. and She, G.L. (2023), "Wave propagation in double nano-beams in thermal environments using the Reddy's high-order shear deformation theory", *Adv. Nano Res.*, **14**(6), 495-506. https://doi.org/10.12989/anr.2023.14.6.495.
Xiao, L. (2023), "Hybrid adaptive neuro-fuzzy inference system method for energy absorption of nano-composite reinforced beam with piezoelectric face-sheets", *Adv. Nano Res*., **14**(2), 141-154. https://doi.org/10.12989/anr.2023.14.2.141.
Xu, J.Q. and She, G.L. (2023), "Thermal post-buckling and

primary resonance of porous functionally graded beams: Effect of elastic foundations and geometric imperfection", *Comput. Concrete*, **32**(6), 543-551. https://doi.org/10.12989/cac.2023.32.6.543.

Yaylaci, E.U., Oner, E., Yaylaci, M., Ozdemir, M.E., Abushattal, A. and Birinci, A. (2022a), "Application of artificial neural networks in the analysis of the continuous contact problem", *Struct. Eng. Mecha.*, **84**(1), 35-48. https://doi.org/10.12989/sem.2022.84.1.035.

Yaylaci, E.U., Ozdemir, M.E., Guvercin, Y., Ozturk, S. and Yaylaci, M. (2023a), "Analysis of the mechano-bactericidal effects of nanopatterned surfaces on implant-derived bacteria using the FEM", *Adv. Nano Res.*, **15**(6), 567-577. https://doi.org/10.12989/anr.2023.15.6.567.

Yaylaci, E.U., Yaylaci, M., Ozdemir, M.E., Terzi, M. and Ozturk, S. (2023b), "Analyzing the mechano-bactericidal effect of nano-patterned surfaces by finite element method and verification with artificial neural networks", *Adv. Nano Res*, **15**(2), 165-174. https://doi.org/10.12989/anr.2023.15.2.165.

Yaylaci, M. (2016), "The investigation crack problem through numerical analysis", *Struct. Eng. Mech.*, **57**(6), 1143-1156. https://doi.org/10.12989/sem.2016.57.6.1143.

Yaylaci, M. (2022), "Simulate of edge and an internal crack problem and estimation of stress intensity factor through finite element method", *Adv. Nano Res.*, **12**(4), 405-414. https://doi.org/10.12989/anr.2022.12.4.405

Yaylaci, M. and Avcar, M. (2020), "Finite element modeling of contact between an elastic layer and two elastic quarter planes", *Comput. Concrete,* **26**(2), 107-114. https://doi.org/10.12989/cac.2020.26.2.107.

Yaylaci, M., Abanoz, M., Yaylacı, E.U., Olmez, H., Sekban, D.M. and Birinci, A. (2022b), "Evaluation of the contact problem of functionally graded layer resting on rigid foundation pressed via rigid punch by analytical and numerical (FEM and MLP) methods", *Arch. Appl. Mech.*, **92**, 1953-1971. https://doi.org/10.1007/s00419-022-02159-5.

Yaylaci, M., Abanoz, M., Yaylaci, E.U., Olmez, H., Sekban, D.M. and Birinci, A. (2022c), "The contact problem of the functionally graded layer resting on rigid foundation pressed via rigid punch", *Steel Compos. Struct.*, **43**(5), 661-672. https://doi.org/10.12989/scs.2022.43.5.661.

Yaylaci, M., Öner, E., Adıyaman, G., Öztürk, Ş., Uzun Yaylaci, E., and Birinci, A. (2023c), "Analyzing of continuous and discontinuous contact problems of a functionally graded layer: theory of elasticity and finite element method", *Mech. Based Des. Struct. Machines*, **52**(8), 5720-5738. https://doi.org/10.1080/15397734.2023.2262562.

Yaylaci, M., Sabano, B.S., Ozdemir, M.E. and Birinci, A. (2022d), "Solving the contact problem of functionally graded layers resting on a HP and pressed with a uniformly distributed load by analytical and numerical methods", *Struct. Eng. Mech.*, **82**(3), 401-416. https://doi.org/10.12989/sem.2022.82.3.401.

Yaylaci, M., Yaylaci, E.U., Ozdemir, M.E., Ay, S. and Ozturk, S. (2022e), "Implementation of finite element and artificial neural network methods to analyze the contact problem of a functionally graded layer containing crack", *Steel Compos. Struct.*, **45**(4), 501-511. https://doi.org/10.12989/scs.2022.45.4.501.

Yaylaci, M., Yaylaci, E.U., Ozdemir, M.E., Ozturk, S. and Ssli, H. (2023d), "Vibration and buckling analyses of FGM beam with edge crack: Finite element and multilayer perceptron methods", *Steel Compos. Struct.*, **46**(4), 565-575. https://doi.org/10.12989/scs.2023.46.4.565.

Yaylaci, M., Yayli, M., Yaylaci, E.U., Olmez, H. and Birinci, A. (2021), "Analyzing the contact problem of a functionally graded layer resting on an elastic half plane with theory of elasticity, finite element method and multilayer perceptron", *Struct. Eng. Mech.*, **78**(5), 585-597. https://doi.org/10.12989/sem.2021.78.5.585

Zerrouki, R., Hamidi, A., Tlidji, Y., Karas, A., Zidour, M. and Tounsi, A. (2022), "Free vibration responses of nonlinear FG-CNT distribution in a polymer matrix", *Smart Struct. Syst.*, **30**(2), 135-143. https://doi.org/10.12989/sss.2022.30.2.135.

Zerrouki, R., Karas, A., Zidour, M., Bousahla, A.A., Tounsi, A., Bourada, F., Tounsi, A., Benrahou, K.H. and S.R. Mahmoud, (2021), "Effect of nonlinear FG-CNT distribution on mechanical properties of functionally graded nanocomposite beam", *Struct. Eng. Mech.*, **78**(2), 117-124. https://doi.org/10.12989/sem.2021.78.2.117.

Zhai, Y., Yu, X., Yue, X., Wang, P. and Zhang, P. (2021), "Dynamic property of functionally graded carbon nanotube-reinforced composite plates with viscoelastic core", *Compos. Struct.,* **275**, 114466. https://doi.org/10.1016/J.COMPSTRUCT.2021.114466.

Zhang, Y., Guo, Z., Gong, Y., Shi, J., El Ouni, M.H. and Alhosny, F. (2023a), "Elastic buckling performance of FG porous plates embedded between CNTRC piezoelectric patches based on a novel quasi 3D-HSDT in hygrothermal environment", *Adv. Nano Res.*, **15**(2), 175-189. https://doi.org/10.12989/anr.2023.15.2.175.

Zhang, Y., Zhang, B., Shen, H., Wang, Y., Zhang, X. and Liu, J. (2020), "Nonlinear bending analysis of functionally graded CNT-reinforced shallow arches placed on elastic foundations", *Acta Mechanica Solida Sinica*., **33**, 164-186. https://doi.org/10.1007/s10338-019-00141-3.

Zhang, Y.W., Ding, H.X., She, G.L. and Tounsi, A. (2023b), "Wave propagation of CNTRC beams resting on elastic foundation based on various higher-order beam theories", *Geomech. Eng..,* **33**(4), 381-391. https://doi.org/10.12989/gae.2023.33.4.381.

Zhu, Y. (2023), "Critical multi-field load analysis of the piezoelectric/piezomagnetic microplates as an application in sports equipment", *Adv. Nano Res.*, **15**(5), 485-493. https://doi.org/10.12989/anr.2023.15.5.485.

CC